

DTIC FILE COPY

12

AD

AD-E 401 739

Contractor Report Number ARAED-CR-87024

NOVEL ANALYTICAL X-RAY NON-DESTRUCTIVE EVALUATION (NDE)  
TOOL FOR QUALITY CONTROL OF ENERGETIC MATERIALS

AD-A187 737

Dr. Ronald G. Rosemeier  
T.S. Ananthanarayanan  
Dr. Sudhir B. Trivedi  
Alfred L. Wiltout  
Douglas C. Leepa  
Bruce E. Harrison  
Jolanta I. Soos  
Brimrose Corporation of America  
7720 Belair Road  
Baltimore, MD 21236

DTIC  
ELECTED  
NOV 06 1987  
S D

James Pinto  
Project Engineer  
ARDEC

( 12 OCT 1987 )



US ARMY  
ARMAMENT RESEARCH,  
DEVELOPMENT AND  
ENGINEERING CENTER

U.S. ARMY ARMAMENT RESEARCH, DEVELOPMENT AND  
ENGINEERING CENTER

Armament Engineering Directorate  
Picatinny Arsenal, New Jersey

Approved for public release; distribution unlimited.

87 10 20 074

The views, opinions, and/or findings contained in this report are those of the author(s) and should not be construed as an official Department of the Army position, policy, or decision, unless so designated by other documentation.

The citation in this report of the names of commercial firms or commercially available products or services does not constitute official endorsement by or approval of the U.S. Government.

Destroy this report when no longer needed by any method that will prevent disclosure of contents or reconstruction of the document. Do not return to the originator.

## REPORT DOCUMENTATION PAGE

1a. REPORT SECURITY CLASSIFICATION		1b. RESTRICTIVE MARKINGS	
2a. SECURITY CLASSIFICATION AUTHORITY		3. DISTRIBUTION/AVAILABILITY OF REPORT APPROVED FOR PUBLIC RELEASE; DISTRIBUTION UNLIMITED	
2b. DECLASSIFICATION/DOWNGRADING SCHEDULE			
4. PERFORMING ORGANIZATION REPORT NUMBER(S)		5. MONITORING ORGANIZATION REPORT NUMBER(S) ARAED-CR-87024	
6a. NAME OF PERFORMING ORGANIZATION Brimrose Corp. of America	6b. OFFICE SYMBOL (If applicable)	7a. NAME OF MONITORING ORGANIZATION ARDEC, AED	
6c. ADDRESS (City, State and ZIP Code) 7720 Belair Road Baltimore, MD 21236		7b. ADDRESS (City, State and ZIP Code) Energetics and Warheads Div. (SMCAR-AEE-WW) Picatinny Arsenal, NJ 07806-5000	
8a. NAME OF FUNDING/SPONSORING ORGANIZATION ARDEC, IMD	8b. OFFICE SYMBOL (If applicable)	9. PROCUREMENT INSTRUMENT IDENTIFICATION NUMBER DAAA21-86-C-0271	
8c. ADDRESS (City, State and ZIP Code) STINFO Br (SMCAR-IMI-I) Picatinny Arsenal, NJ 07806-5000		10. SOURCE OF FUNDING NOS.	
		PROGRAM ELEMENT NO.	PROJECT NO.
		TASK NO.	WORK UNIT NO.
11. TITLE (Include Security Classification) Novel Analytical X-ray Non-Destructive (NDE) Tool for Quality Control of Energetic Materials			
12. PERSONAL AUTHOR(S) R. G. Rosemeier, T. S. Ananthanarayanan, S. B. Trivedi, A. L. Wiltrout, D. C. Leepa, B. Harrison, J. I. Soos, Brimrose Corp., J. Pinto, Project Engineer, ARDEC			
13a. TYPE OF REPORT FINAL	13b. TIME COVERED FROM 8/28/86 TO 2/28/87	14. DATE OF REPORT (Yr., Mo., Day) 10/05/87	15. PAGE COUNT
16. SUPPLEMENTARY NOTATION			
17. COSATI CODES		18. SUBJECT TERMS (Continue on reverse if necessary and identify by block number)	
FIELD	GROUP	SUB. GR.	
			RDX, HMX, explosives, propellants, quality control, real time, x-ray
19. ABSTRACT (Continue on reverse if necessary and identify by block number)			
<p>Particle size, segregation and composite homogeneity are some of the critical parameters affecting propellant performance. Several investigations have been undertaken to resolve this issue. The current study involves the use of real time x-ray diffraction experiments to quantify the above mentioned parameters.</p> <p>2-D x-ray detectors in combination with state-of-the-art image processing hardware/software have significantly enhanced the analytical capabilities. Several composites and simulants have been examined using these techniques. A procedure for x-ray "finger printing" individual constituents in composites has been successfully implemented. Algorithms have also been developed for particle size and distribution analysis. Some of the initial results have been presented to show the efficacy of such techniques in rapid on-line production oriented applications. Additionally, these techniques can also be used to determine micro-lattice strain states in various constituents in the composites.</p> <p>All x-ray methods used are firmly based on 1st principles (Bragg's Law of x-ray diffraction). Integration with digital imaging and advanced computing techniques makes expert system design viable and extremely lucrative for production feed back control.</p>			
20. DISTRIBUTION/AVAILABILITY OF ABSTRACT UNCLASSIFIED/UNLIMITED <input checked="" type="checkbox"/> SAME AS RPT. <input type="checkbox"/> DTIC USERS <input type="checkbox"/>		21. ABSTRACT SECURITY CLASSIFICATION Unclassified	
22a. NAME OF RESPONSIBLE INDIVIDUAL I. Haznedari (STINFO's) point of contact with DTIC)	22b. TELEPHONE NUMBER (Include Area Code) AV880-3316	22c. OFFICE SYMBOL SMCAR-IMI-I	

**CONTENTS**

	<b>PAGE #</b>
Introduction	1
Technical Approach	2
X-ray Diffractometry, Powder Diffraction Rocking Curve Topography	
Results and Discussion	4
Micro-lattice Strain Measurements	
Propellant Mixing and Distribution	
Solid Propellant Characterization Constituent Phase Analysis Real Time Particle Size & Phase Analysis	
Process Induced Damage in Propellants	
Phase I Conclusion	6
Future Directions: Novel Concept in X-ray Powder Analysis	7
References	8
Distribution List	



Accession For	
NTIS CRA&I	<input checked="" type="checkbox"/>
DTIC TAB	<input type="checkbox"/>
Unannounced	<input type="checkbox"/>
Justification	
By	
Distribution/	
Availability Codes	
Dist	Avail and/or Special
<b>A-1</b>	

## LIST OF FIGURES

	PAGE #
1 PIXI Portable Image X-ray Intensifier	10
2 DIXIE Digital Intensity X-ray Image Enhancer.	10
3 Geometry of Conventional X-ray Diffractometer from Cullity, B. D., "Elements of X-ray Diffraction," Addison-Wesley Publishing Co. Inc., Reading MA.	11
4 Diffraction Geometry for White Beam Rocking Curve Topography.	11
5a Schematic of a Digital Rocking Curve Analyzer.	12
5b Digital Automated Rocking Curve Topography.	13
5c Digital Automated Rocking Curve Topography.	13
6 NaCl White Rocking Curve Topography Cu Radiation (510) Reflection, Surface Orientation (100), 2-Theta = 57.225, Incidence Angle $\approx 3^\circ - 4^\circ$ , $\Delta\theta$ (Angular Increment) between Frames = $0.10^\circ$ .	14
7 NaCl Hardness Indentation (222) Reflection Perspective of Rocking Curve Topograph.	15
8 ZnCdTe Epi/InSb (111), 010 Reflection, Cu Radiation (white).	15
9 Rapid X-ray Diffraction Pattern of HMX and RDX.	16
10 Showing Partial X-ray Diffraction Profiles to RDX & HMX with Appropriate Windows for Constituent Phase Identification and Composition Analysis.	17
11 Schematic of Proposed System.	17
12a Real Time Laue Diffraction Pattern from Sugar Particles 74-149 $\mu$ m.	18
12b Real Time Laue Diffraction Pattern from Sugar Particles 44-74 $\mu$ m.	19
12c Real Time Laue Diffraction Pattern from Sugar Particles 0-44 $\mu$ m.	20
13a Real Time Transmission Laue of Several Propellant Composites, 74 $\mu$ m RDX, RDX and Al Composites in PBX, 10% Al/HTPB Composite.	21
13b Real Time Laue Transmission of RDX and Al Composites with Al Foil.	22

13c	Schematic of Real Time Transmission Laue.	23
14	Real Time Transmission Laue of Al Foil.	24
15	Real Time Transmission Laue of Al, Cu, Brass, Ni Foils.	24
16a	Effect of Crushing on Pure RDX (Cr Radiation).	25
16b	Production RDX (Lot X661) US. Pure RDX.	26
16c	Production RDX (Lot A597) US. Pure RDX.	27
16d	Production RDX (Lot A984) US. Pure RDX.	28
16e	RDX Sample Lot 78 (Cr Radiation).	29
17	Formation of X-ray (Debye-Scherrer) Powder Pattern in a Cylindrical Camera.	30
18	Improved Real Time Powder Diffraction Technique.	30

## INTRODUCTION

Factors affecting the stability of energetic materials are not well understood. Knowledge of these factors is essential for the predictability and hence the successful applications of energetic materials as explosives and/or propellants. This in turn involves study of energetic reactions and reaction parameters. The effects of lattice defects, particle size, temperature, radiation and mechanical impact on the initiation and subsequent propagation of solid-state decomposition reaction have been studied by several researchers. (refs 1 through 11). However, the identification and understanding of factors governing energetics in these reactions is not achieved as of yet. This problem in our opinion can be understood in terms of the microstructure of these materials. This report focuses on the study of microstructure of energetic materials using novel non-destructive, non-intrusive x-ray diffraction techniques developed at Brimrose.

The term "micro-structure" is used in the metallurgical sense meaning "the study of the perfection/imperfection in the crystal lattice." Conventional as well as novel x-ray diffraction techniques have been used to quantify the "micro-structure." The materials on which these studies have been carried out include RDX/HMX composites, Ammonium Perchlorate (AP), Aluminum (Al), RDX/Al in PBX, AP/Al in PBX and AP in HTPB elastomeric binders. Work on other materials is also included for the sake of completeness.

The reported study is divided into three major categories:

- 1) Measurement of micro-lattice strains (single crystal)
- 2) Micro-structural study of various mixtures of energetic materials and/or simulants (polycrystalline aggregates)
- 3) Evaluation of process induced damage.

The current effort has its major emphasis on the use of real time quantitative x-ray diffraction techniques for rapid quality control of crystalline solid propellants. These techniques are non-destructive and non-contacting in nature. Presently, the speed of analysis is limited by the intensity of the x-ray source and the computing machinery utilized. All the x-ray techniques discussed in this report have been successfully implemented in real time (30ms) or near real time (few seconds). This study has resulted in the development of an x-ray quality control tool for production applications and much needed quantitative tool for advanced research environments.

The Phase I effort has shown the effect of processing damage on RDX. Process induced damage modifies the microstructure and hence the properties of propellants. The Phase I effort has also clearly highlighted the importance of the incident signal intensity. Currently this factor predominantly limits the on-line capability of the system. The Phase II study will overcome this barrier by incorporating a high intensity x-ray source in the system. In combination with monochromators, 2-D x-ray image detectors powerful computing machinery. These techniques can then be implemented in on-line production applications.

## TECHNICAL APPROACH

X-ray diffraction (refs 1 through 11) has been successfully used as a Quality Control/Quality Assurance tool for several decades now. Historically, photographic film was used to record x-ray diffraction events. These techniques are cumbersome and tedious to use. Using nuclear track plates (photographic emulsions on glass plates) the spatial resolution limit of the photographic technique is in the vicinity of 1-3 $\mu$ m. Digitization of photographic data is very time consuming. Typically, this is done using photo densitometers to measure the gray shades in the film. Data thus collected is digitized by computers.

The use of electronic detectors to directly record x-ray diffraction phenomena has become an increasingly attractive alternative. These detectors range from point counters to 2-dimensional x-ray array detectors. The current emphasis is on the 2-dimensional real time x-ray imaging system that was pioneered by Green et. al. (refs 13 through 14) at Johns Hopkins University. This group of investigators has been successfully utilizing the x-ray image tube to register real time x-ray diffraction events (ref 15). Rosemeier et. al. (ref 16) have used the x-ray image tube to study laser induced microstructural damage. Ananthanarayanan et. al., (ref 17) have successfully integrated the x-ray image tube with an image processor to obtain digital real time x-ray images. Figure 1 shows a three stage, first generation x-ray image intensifier used by the above mentioned investigator. Figure 2 depicts the DIXIE (Digital Intensity X-ray Image Enhancer).

### X-ray Diffractometry, Powder Diffraction

There are two distinct x-ray diffractometric techniques:

- a. Conventional x-ray diffractometry
- b. Double crystal x-ray diffractometry (rocking curve analysis)

Figure 3 shows the x-ray optics and geometry of the conventional diffractometer. Here the essential principle is that the specimen and detector rotate about the diffractometer axis with  $\theta$ - $2\theta$  angular velocity relationship. This coupled rotation minimizes errors due to change in absorption factors with incidence angle.

The first crystal being the monochromator and the second crystal (of the "double") is the crystal to be analyzed. In contrast to conventional diffractometry, here the detector is fixed as the sample is rocked (oscillated) about the diffractometer axis. Also known as rocking curve diffractometry, this technique has been used by several investigators (ref 18) with point counters (ref 19) and linear position sensitive detectors (ref 20) to study materials and microstructural morphologies. The detector can be positioned (fixed) at any two-theta value and the diffraction domain probed by rocking the specimen about the diffractometer axis.

## Rocking Curve Topography

Rocking curve topography is the implementation of double crystal diffractometry in 2-dimensions i.e., the incident beam is 2-dimensional and the detector used is a 2-dimensional array detector. Typical incident beam size and diffraction geometry are illustrated in Figure 4. This technique can be used with:

- a. White incident beam
- b. Monochromated incident beam ( $n$ ,  $-n$  or  $n$ ,  $+n$  setting)

This study utilizes the former and is called White Rocking Curve Topography. No attempt is made to monochromate the incident beam. A 0.6 kW conventional Cu x-ray source containing  $K_{\alpha 1}$ ,  $K_{\alpha 2}$  and  $K_{\beta}$  components along with some fraction of the Brehmstrahlung was used as an incident beam. A line source was used to maximize sampling area. Grazing incidence angle of  $(1-5^{\circ})$  was used to irradiate the entire specimen area. The specimen was mounted on a high precision multi-axis, computer controlled goniometer. This sample manipulation system allows the probing of the entire reciprocal space volume to determine and optimize the required diffraction topographs. There are typically 6 degrees of freedom on the specimen goniometer. The translation resolution of the actuators is 0.1  $\mu\text{m}$  and the angular resolution of the rotary stages is 0.1 arc sec. The individual actuators are equipped with optical encoders to minimize, if not eliminate, backlash and other related errors. A detailed schematic of the entire rocking curve topography system is depicted in Figure 5a-c.

Some of the pioneering work on rocking curve analysis was done by Weissmann (ref 21) et. al. at Rutgers University using a linear position sensitive detector (ref 22). Ananthanarayanan (ref 23) et. al. at Brimrose Laboratories have significantly enhanced this technique by successfully integrating a 2-dimensional detector in the system. Thus, it is now feasible to obtain 2-dimensional rocking curve topographs (maps), integrated intensity maps and peak shift maps of 1.5" diameter area in less than 3 secs. The spatial resolution of this technique is currently 100-150  $\mu\text{m}$  and the angular resolution is fractions of arc seconds. With CCD's (charge couple devices) the spatial resolution is improved to 20-25  $\mu\text{m}$ . The dynamic range of the existing CCD's is about 16,000:1. The use of quality control techniques as discussed here will perhaps some day lead to CCD's with resolution comparable to those obtainable with nuclear track plates.

Rocking curve analysis involves the measurement of the FWHM (full width at half maxima) of individual Bragg diffraction spots. By oscillating the analyzed crystal about the diffractometer axis through its diffracting domain, the entire reciprocal volume can be recorded. The FWHM measured thus is a function of the local dislocation density. Hersch et. al. (ref 24) showed this relation to be  $\rho = \beta^2 / 2b$  where,  $\beta$  - FWHM,  $\rho$  - dislocation density,  $b$  - Bergers vector. Dinan et. al. (ref 25) have clearly shown the utility of the rocking curve technique for the characterization of various substrates and epitaxial films used in micro-electronics applications. These investigators used a point counter in their experiments.

In the present study both 1-D and 2-D x-ray sources were used. Topographic images were obtained by scanning the specimen surface with the 1-D x-ray beam while no such translation was required in the case of the 2-D x-ray beam and 2-D detector combination.

## RESULTS AND DISCUSSIONS

### Micro-lattice Strain Measurements

Figure 6 shows the (222) rocking curve analysis from a NaCl crystal with a Brinell hardness indentation. This indentation was made with a 20kg preload. The Bragg peak broadening (perspective view) shown in Figure 7 clearly depicts the dislocation morphology around the indentation. The strain anisotropy along the (110) directions can also be seen. In contrast to the rocking curve half width map, the peak shift map has little correlation with the hardness indentation. This is reasonable because the effect of the indentation on the lattice parameter map (Bragg peak shift map) is minimal.

Figure 8 depicts the rocking curve topograph from a ZnCdTe epitaxy/InSb substrate grown by MBE. This topograph shows dislocation striations formed either by the growth process and/or by twinning in the substrate. These striations have definite crystallographic orientation. Further analysis is required to accurately determine the origin of this morphology.

The  $\text{Cd}_{0.95}\text{Zn}_{0.05}\text{Te}$  layers were grown by MBE on {100} InSb substrate. Composition of the alloy layers was set by adjusting the temperatures of two effusion cells, one containing polycrystalline CdTe, other, elemental Zn. Additional details of substrate surface preparation and growth conditions are given elsewhere (ref 26).

In conclusion DARC topography technique provides quantitative information about the micro-lattice strain inhomogeneities in various crystalline materials. These maps of the Bragg peak shift, Bragg peak broadening can be translated to appropriate micro-lattice strain maps. The integrated intensity under each pixel can also be used to determine epitaxial film thickness. The DARC technique is highly amenable to automation and on-line production applications.

### Propellant Mixing & Distribution

Solid Propellant Characterization. During the preliminary phases of the investigations of pure RDX and HMX, x-ray diffraction spectra were acquired. Examples of the x-ray spectra of both pure RDX and pure HMX are shown in Figure 9 along with a typical production grade sample of RDX. These spectra are unique to the phases and the relative intensity of each spectrum is indicative of the amount of the constituent phases.

The method presented here can provide a point by point determination of several important parameters of a solid propellant casing cross section. These include:

- a.) relative amounts of RDX, HMX and Al powders
- b.) particle size.

By comparison of adjacent regions, this information can be used to study agglomeration of the individual phases throughout the cross-section. This information will permit a thorough analysis of the effect of particle size on the non-uniform distribution of the solids and their tendency to agglomerate.

The method utilized here is based on the ability to collect x-ray diffraction spectra on a point by point basis throughout a large specimen area and then to be able to correlate this spectra to the constituents within the small volume giving rise to the diffraction event. Thus, there are two main concerns which this study addresses:

- a.) the ability to scan the x-ray probe over a large specimen area with a spot size in the range of 1mm diameter and
- b.) the ability to correlate the collected diffracted spectra with the properties of interest, namely volume fraction and particle size of the constituents.

This x-ray method employs a conventional x-ray diffraction unit modified in several important ways for the current application. These include the use of a position sensitive detector (PSD) and 2-D detectors. The use of digital detectors and the computer permits a much more rapid analysis than would ordinarily be expected. The use of a small incident beam and scanning of the sample would permit mapping of the important material parameters throughout the sample with high spatial resolution.

#### Constituent Phase Analysis

The operating principle of the method is based on the diffraction spectra of pure RDX and pure HMX shown in Figure 9. As mentioned previously, these spectra are unique to each phase and the intensity of the spectra is roughly proportional to the amount of the individual phase. Thus, in a sample representing a mixture of the two phases, the measurement of the relative intensities of the unique peaks permits a calculation of the volume fraction. This is shown in Figure 10, which is a region of the two unique spectra, enlarged for clarity. Also, shown in this figure are two regions of interest (or windows). Note that in the first window, centered at about  $22^\circ$  that the diffraction peak for HMX is quite strong while the peak for RDX is absent. Similarly, in the second window, centered at about  $38^\circ$ , the RDX peak is strong while the HMX peak is absent.

The windows cited above can be easily followed with the aid of a Position Sensitive Detector (PSD) as the detector element. Such a device permits the simultaneous observation of a large angular range. Thus, two windows mentioned above can be easily monitored and the total diffracted intensity within that window can be determined. Moreover, there is no fundamental restriction as to how many windows can be created. Thus, it is possible to create a large number of windows which can be used to monitor the unique signals coming from any additional phase, such as powdered aluminum.

The operating sequence for the above method is shown in Figure 11. The sample is held stationary while a small, well collimated x-ray beam impinges on a region 1mm diameter. The resulting x-ray diffraction profile is collected over the full angular range of the position sensitive detector. When the diffracted intensity is sufficient for a reliable analysis, the profiles are transmitted to the dedicated microcomputer for analysis. While the data is undergoing analysis, the sample is translated 1mm so that the next region is brought into the incident x-ray beam. The process is then repeated until all of the sample surface has been examined.

#### Real Time Particle Size and Phase Analysis

Laue x-ray diffraction technique has been successfully used to study thin discs of propellant composites. Using a 2-D x-ray detector several discs of propellant composites containing RDX, Al, AP, HMX in elastomeric binders (PEX, HTPB) were examined.

These discs were typically 3-5mm in diameter and 0.1-0.5mm thick. Figures 12 & 13 show the Laue diffraction images obtained from various grain size of simulants and actual propellant powder. These images show the effect of particle size on Laue diffraction spots (size, distribution and density). Software will be made available to analyze these images for particle size measurement.

Figure 14 shows the Laue transmission image from an Al foil (Reynold's wrap). Preferred orientation can be observed due to the mechanical rolling that the Al foil was subjected to. Figure 15 depicts the x-ray pattern from a Al, Cu, Brass & Ni foils. These patterns are characteristic of each material and clearly show the polycrystalline nature with preferred orientation or texture due to mechanical rolling in the case of Al. In a sense, they are the microstructural "finger prints" of the individual material (constituent phase). Al & Ni were chosen for this study due to the high signal/noise ratio available with existing x-ray optics for these materials. The limitation for actual propellant was in the intensity of the x-ray source itself. This limitation can be overcome by utilizing higher intensity x-ray source (rotating anode, synchrotron or pulsed x-ray generator).

#### Process Induced Microstructural Damage

Several samples of production grade RDX/HMX mixtures were examined using conventional diffractometry. These results are depicted in Figure 16a-e and were obtained with Cr radiation monochromated by a bent crystal graphite monochromator. Production grade material had similar x-ray diffraction profiles as pure RDX subjected to mechanical grinding (with a mortar & pestle). One sample (lot 78), however, was an exception. These "deformation peaks" have been attributed to stress/strain induced phase transformation products. Further studies have to be conducted with other complimentary techniques to establish this hypothesis and will be a part of continuing investigations.

## PHASE I CONCLUSION

Real time x-ray quantitative techniques have been successfully utilized to characterize single crystals, powder aggregates and paracrystalline composites.

Single Crystal Characterization - using DARC x-ray topography, the surface/sub-surface micro-lattice strain state has been quantified. These topographs yield valuable information about the micro-structure of energetic materials.

Poly-crystalline Aggregates - using real time 2-D x-ray detectors and high speed computers conventional x-ray diffraction techniques can be phenomenally accelerated. With appropriate x-ray signal intensity, these techniques can easily be adapted to production oriented environments. Experiments on "free falling" sugar particles have been very successful and promising.

The current limitation in the analytical tool developed during the Phase I effort is the incident source energy (0.8kW x-ray generator). This limitation reduces the signal to noise ratio. An obvious solution to this impediment is the use of high intensity rotating anode x-ray generator. This type of a generator typically can produce an order of magnitude higher signal, thus allowing monochromation and consequently improving the overall resolution (both temporal as well as spatial) of the techniques.

## FUTURE DIRECTIONS: NOVEL CONCEPT IN X-RAY POWDER ANALYSIS

Conventional x-ray powder cameras (Deby-Scherrer) comprise of a point x-ray source and cylindrical film to record the x-ray patterns. Additionally, the powder sample is rotated about the camera axis throughout the exposure time. The rotation is required to bring various grains into Bragg condition. This film technique inherently integrates all the diffraction events over the exposure time (typically 1-3 hours). The diffraction geometry involved in the above case is shown in Figure 17.

The availability of 2-D real time x-ray detector systems complemented by enormous computing power has facilitated a unique and novel concept in powder analysis. This involves the integration of real time Laue transmission patterns in polar coordinates. This integration is tantamount to rotating the specimen about the transmitted beam direction. However, this integration will require only one 2-D image (33ms exposure time) as opposed to the several hours of exposure in the conventional powder technique. A schematic illustration of this concept is depicted in Figure 18. In addition, the 2-D detector system will allow the recording and storing of standard 2-D diffraction patterns in digital or video format. This opens up a whole new concept in materials data bank. Currently, standard diffraction patterns of various crystalline materials are stored by the JCPDS (Joint Committee for Powder Diffraction Studies, Swarthmore, PA). These data are stored in a tabular form and require enormous storage space for interactive search/match schemes. With the concept of 2-D diffraction spectra, the storage can be accomplished in the video format on a high speed laser disk recorder. It will also allow the customization and periodic updating of the data bank according to user specifications and demands.

## REFERENCES

1. Bowden, F. P., Proc. Roy. Soc. (London) A264 (1958) 146.
2. Elban, W. L. and Armstrong, R. W., 7th Intern. Symp. on Detonation, 1981.
3. Jach, J. S., Nature 196 (1962) 827.
4. Singh, K., Trans. Faraday Soc. 52 (1956) 1623.
5. Bowden, F. P., Stone, M. A. and Tudor, G. K., Proc. Roy. Soc. (London) A188 (1947) 329.
6. Bowden, F. P., Mulcahy, M. F. R., Vines, R. G., and Yoffe, A. D., Proc. Roy. Soc. (London) A188 (1947) 291.
7. Bowden, F. P., Proc. Roy. Soc. (London) A246 (1958) 146.
8. Dick, J. J., J. Appl. Phys. 53 (1982) 6165.
9. Elban W. L., Coffey C. S., Yoc K. C., and Rosemeier R. G., "Microstructural Origins of Hot Spots in RDX Explosive and a Reference Inert Material," NSW MP 84-200, 1984.
10. Coffey C. S., Elban W. L., and Jacobs S. J., "Detection of Local Heating and Reaction Induced by Impact," in Proceedings of the Sixteenth JANNAF Combustion Meeting, Vol. I, 1014 Sep 1979, CPIA Publ. 308, pp. 205-219.
11. Elban W. L., and Armstrong R. W., "Microhardness Study of RDX to Assess Localized Deformation and Its Role in Hot Spot Formation," in Proceedings of the Seventh Symposium (International) on Detonation, 16-19 Jun 1981, NSW MP 82-334, pp. 976-985.
12. Guinier, A., X-ray Diffraction, W. H. Freeman & Co., 1963 ed., San Francisco.
13. Reifsnider, K. and Green Jr., R. E., An Image Intensifier System for Dynamic X-ray Diffraction Studies, Rev. Sci. Instr. 39, 1651, (1968).
14. Green Jr., R. E., Adv. X-ray Anal., 20 (1977) 221.
15. Green Jr., R. E., Boettinger, W. J., Burdette, H. E. and Kuriyama, M., "Asymmetric Crystal Topographic Camera," Rev. Sci. Instrum., Vol. 47, No. 8, August 1976.
16. Rosemeier, R. G. and Allik, T. H., "Characterization of Laser Materials by Real-Time X-ray Topography," The International Conference on Lasers '84 Proceedings, (1984) p. 112.
17. Ananthanarayanan, T. S., Rosemeier, R. G., Mayo, W. E. and Sacks, S., "Novel Non-destructive X-ray Technique for Near Real Time Defect Mapping," submitted at the 2nd International Symposium on the Nondestructive Characterization of Materials, Montreal, Canada (1986).

18. Ananthanarayanan, T. S., Rosemeier, R. G., Mayo W. E. and Becla, P., "Micro Lattice Strain Mapping," Materials Research Society Symposia Proceedings Series, Vol. 90.
19. Halliwell, M. A. G., Lyons, M. H., Tanner, B. K. and Ilczyszyn, P., "Assessment of Epitaxial Layers by Automated Scanning Double Axis Diffractometry," Journal of Crystal Growth 65 (1983) p. 672-678.
20. Mayo, W., Yazici, R., Takemoto, T. and Weissmann, S., XII Congress of Int. Union of Crystallography, 1981, Ottawa, Canada.
21. Reis, A., Slade, J. J. and Weissmann, S., J. Appl. Phys. Vol. 22, p. 655 (1951) Slade Jr., J. J. and Weissmann, S., J. Appl. Phys. Vol. 23, p. 323 (1952).
22. Yazici, R., Mayo, W. E., Takemoto, T. and Weissmann, S., J. Appl. Cryst., 16 (1983) 89.
23. Ananthanarayanan, T. S., Mayo, W. E. and Rosemeier, R. G., "High Resolution Digital X-ray Rocking Curve Topography," submitted at the 35th Annual Denver Conference on Applications of X-ray Analysis, Denver, Colorado (1986).
24. Hersch, P. B., Partridge, P. G. and Segall, R. L., Phil. Mag. Vol. 4, p. 721 (1959).
25. Dinan, J. H., Qadri, S. B., "Evaluation of Substrates of Growth of HgCdTe by Molecular Beam Epitaxy," J. Vac. Sci. Technol. A4 (4), Jul/Aug 1986.
26. Dinan, J. H. and Qadri, S. B., "Thin Solid Films," 131 (1985) 267.

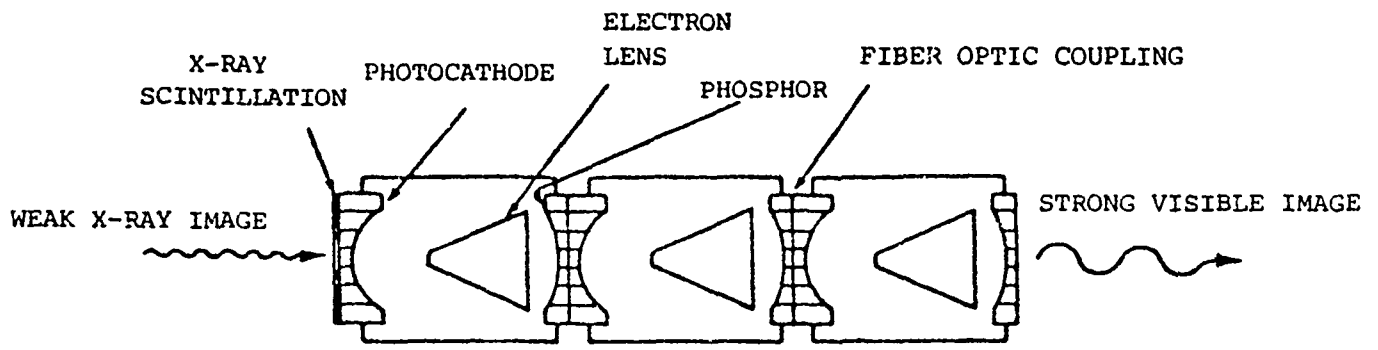


Figure 1 PIXI Portable Image X-ray Intensifier.

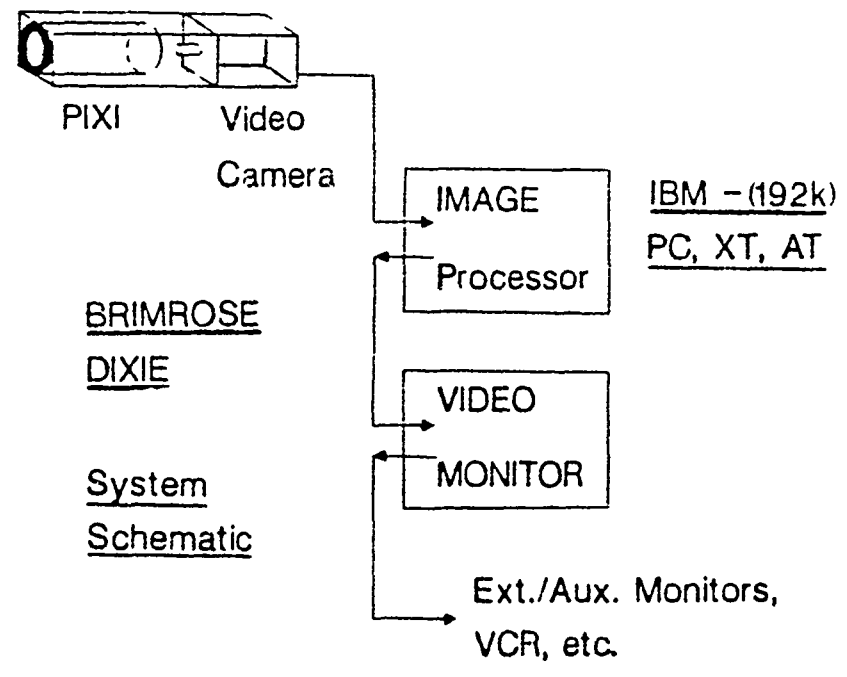


Figure 2 DIXIE Digital Intensity X-ray Image Enhancer.

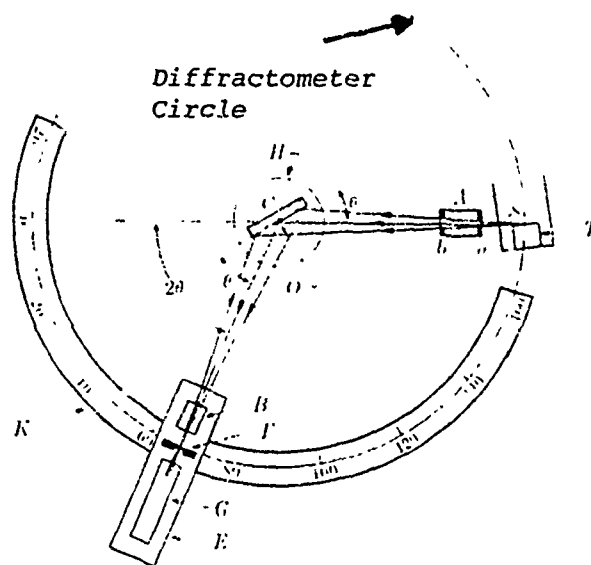


Figure 3 Geometry of Conventional X-ray Diffractometer from Cullity, B. D., "Elements of X-ray Diffraction," Addison-Wesley Publishing Co. Inc., Reading MA.

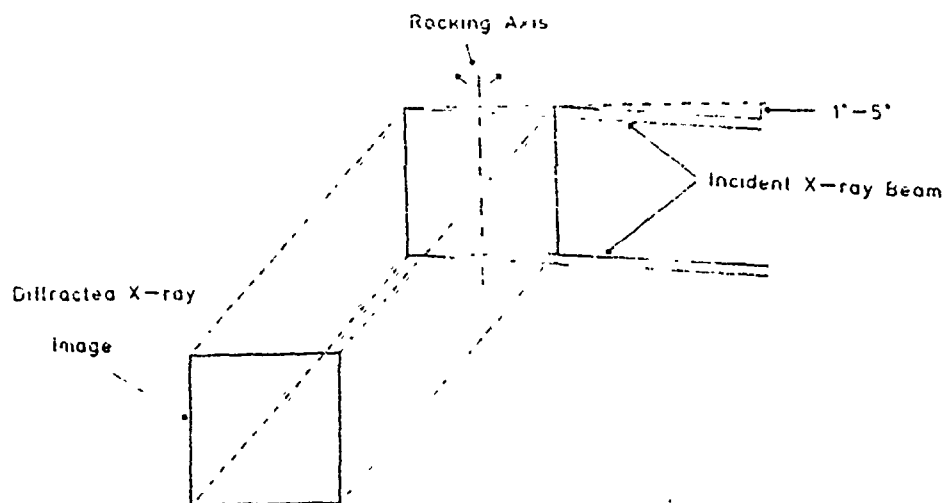


Figure 4 Diffraction Geometry for White Beam Rocking Curve Topography.

# DIGITAL AUTOMATED ROCKING CURVE TOPOGRAPHY

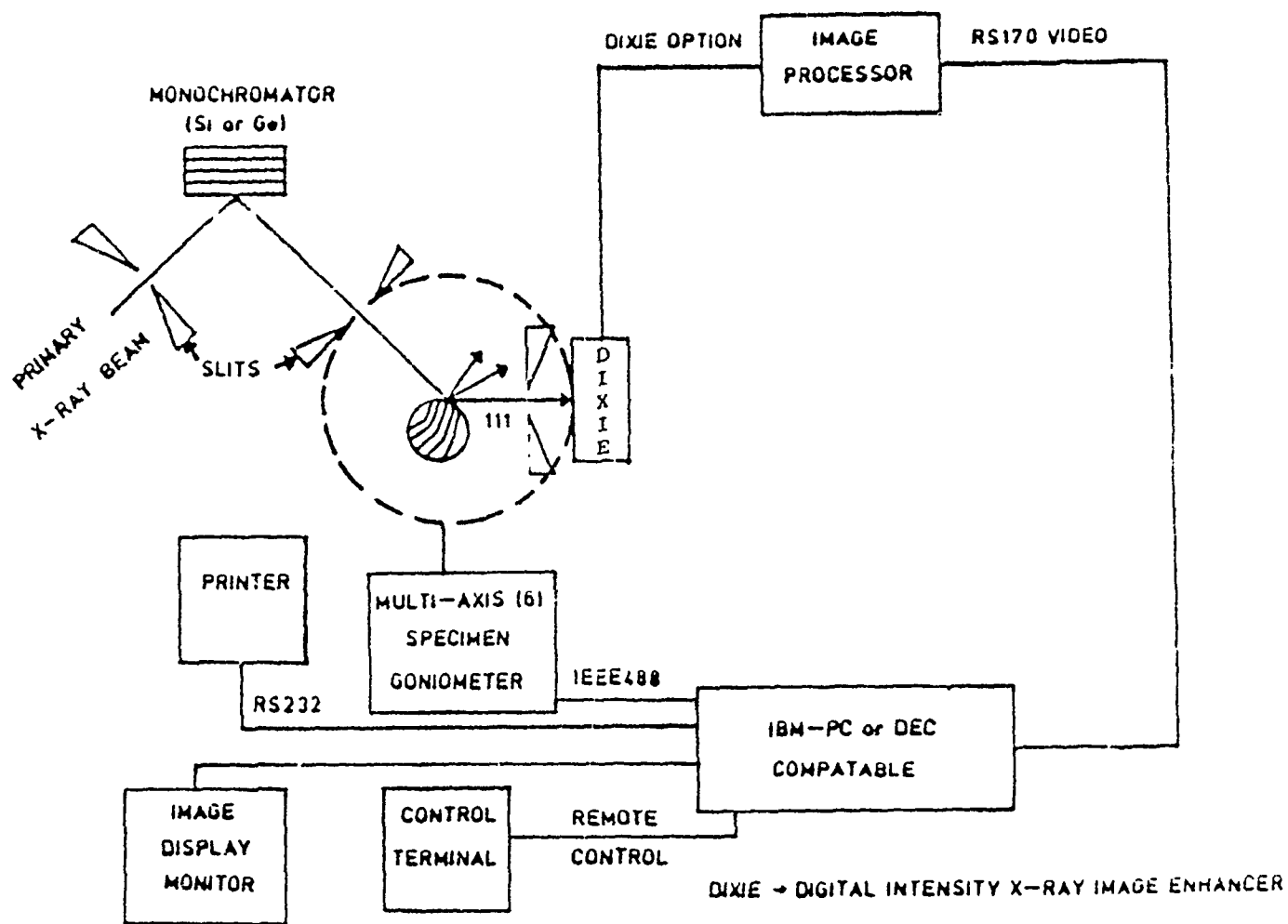


Figure 5a Schematic of a Digital Rocking Curve Analyzer.

# DARC TOPOGRAPHY (DIGITAL AUTOMATED ROCKING CURVE)

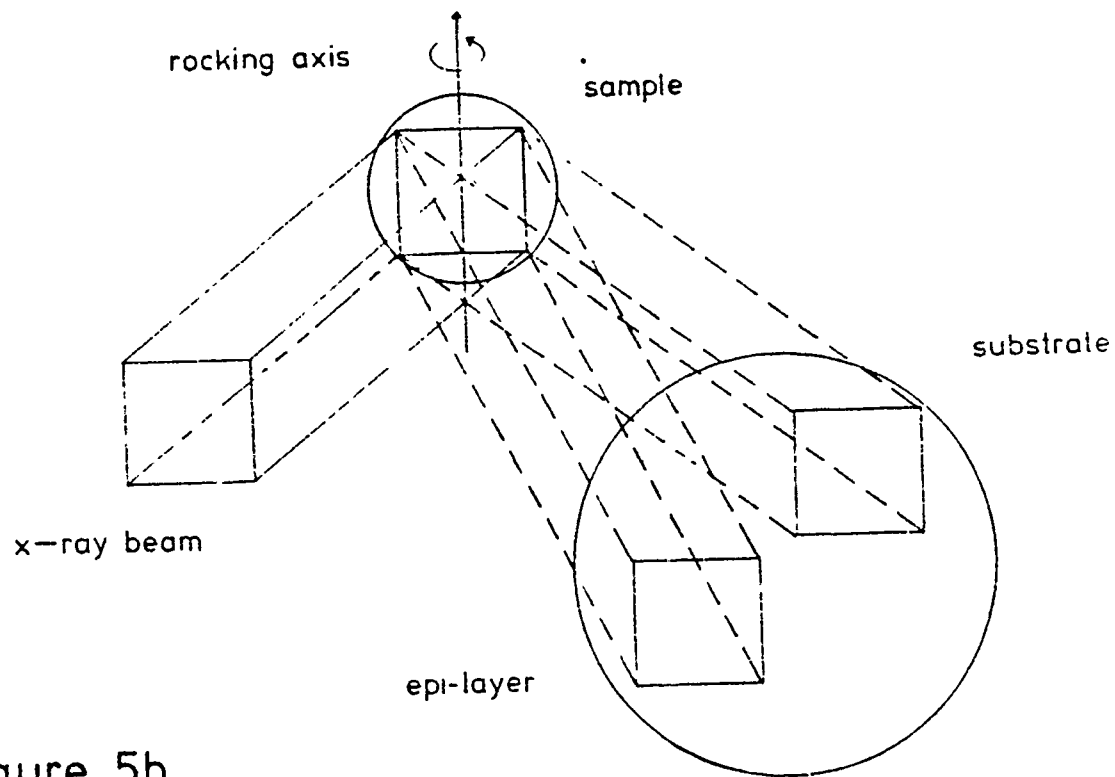


Figure 5b

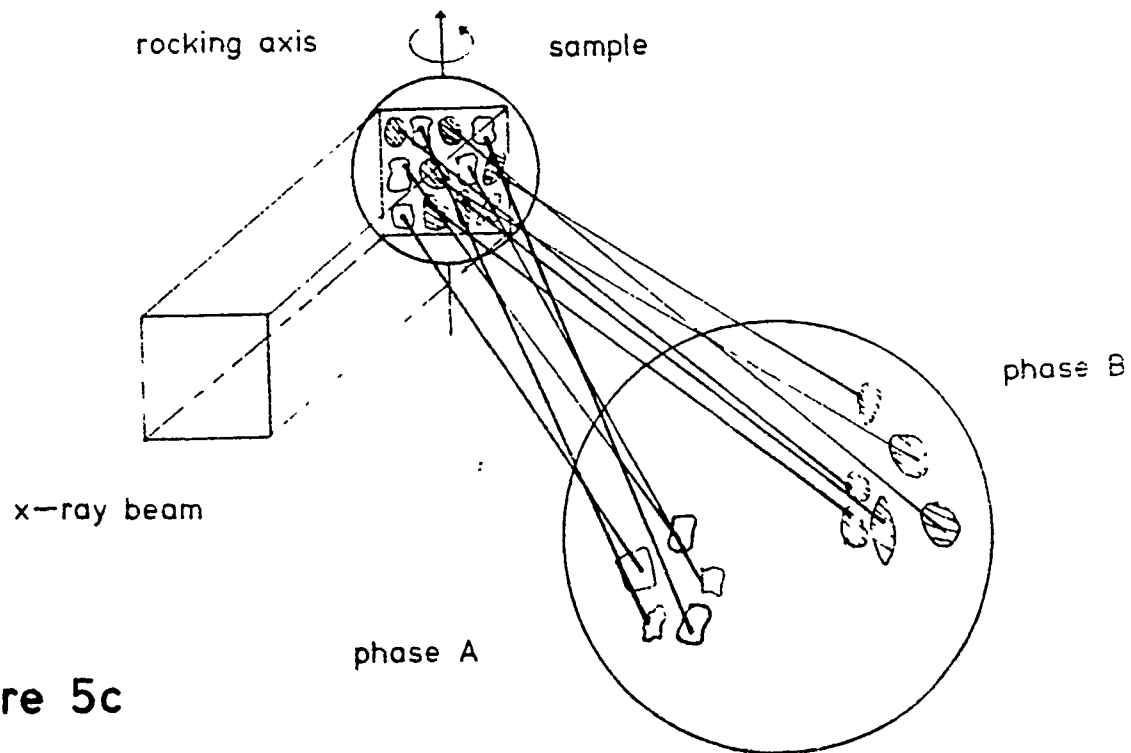


Figure 5c



A. Rocking Curve Raw Data 222 Reflection

B. Bragg Peak Broadening Map



C. Bragg Peak Shift Map



222 Reflection



Figure 6 NaCl White Rocking Curve Topography Cu Radiation (222) Reflection, Surface Orientation (100),  $2\theta = 57.225$ , Incidence Angle  $\approx 3^\circ - 4^\circ$ ,  $\Delta\theta$  (Angular Increment) between Frames  $= 0.10^\circ$ .

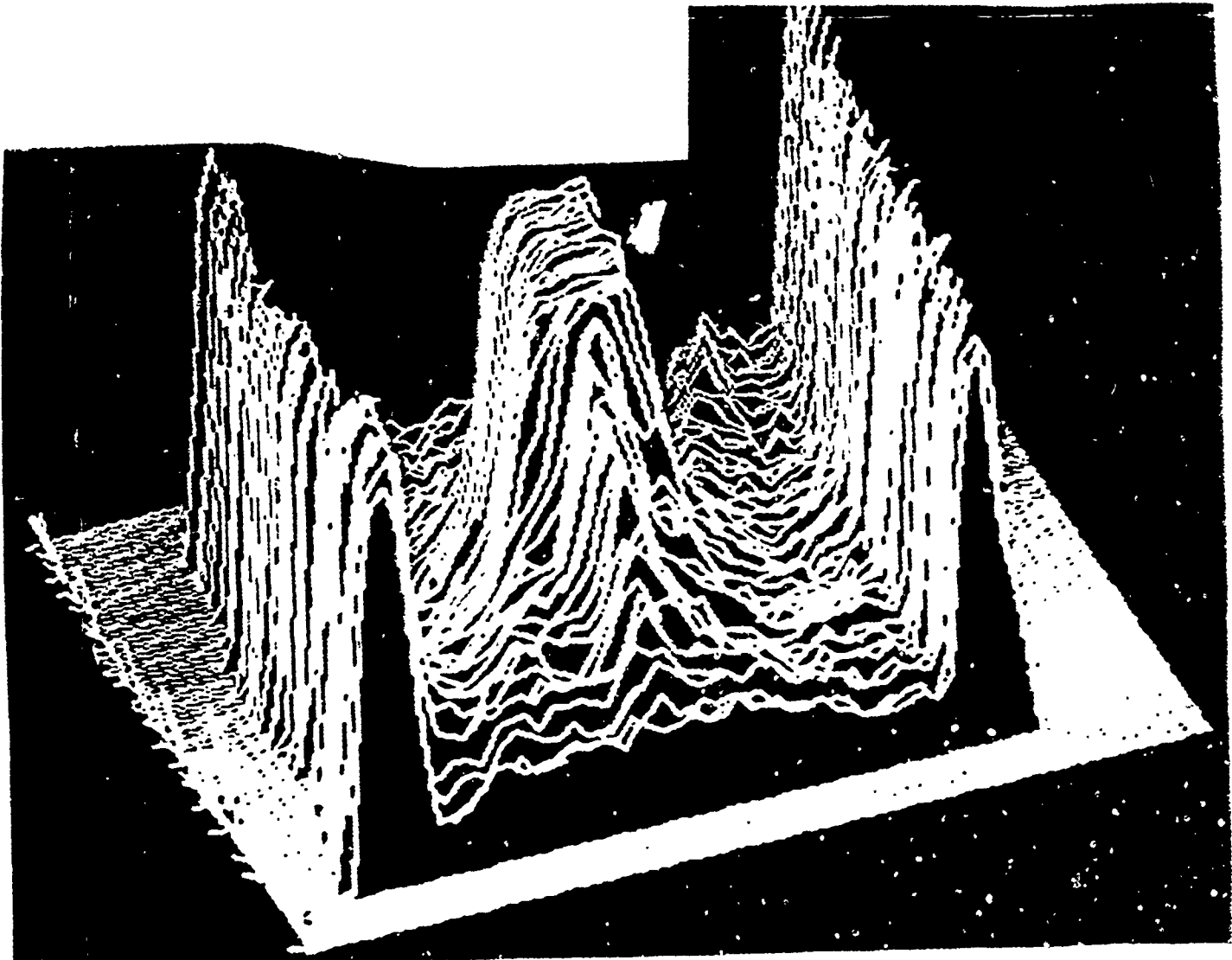


Figure 7 NaCl Hardness Indentation (222) Reflection Perspective of Rocking Curve Topograph.

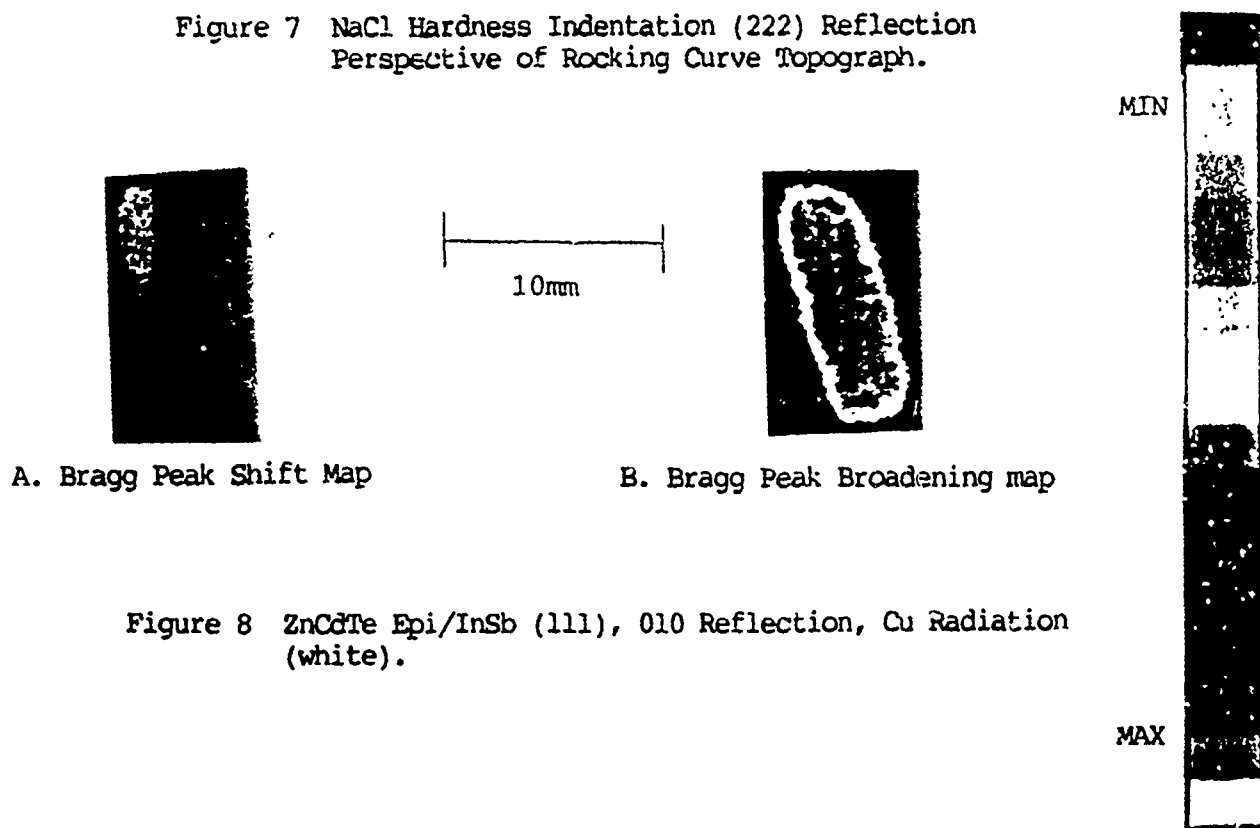


Figure 8 ZnCdTe Epi/InSb (111), 010 Reflection, Cu Radiation (white).

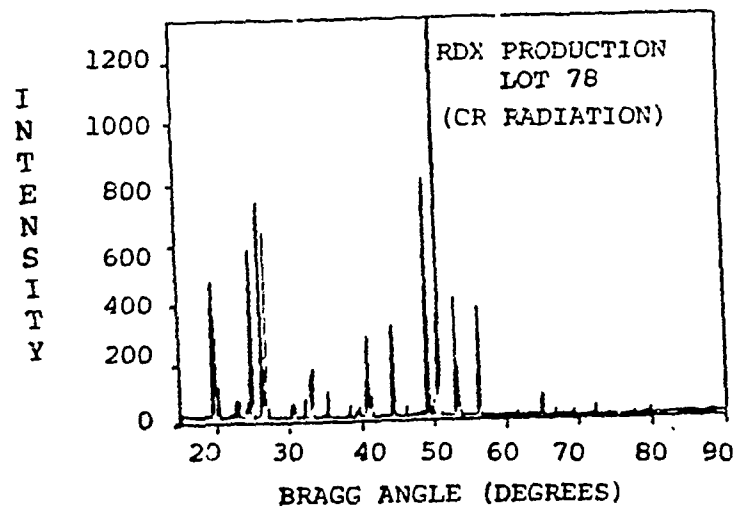
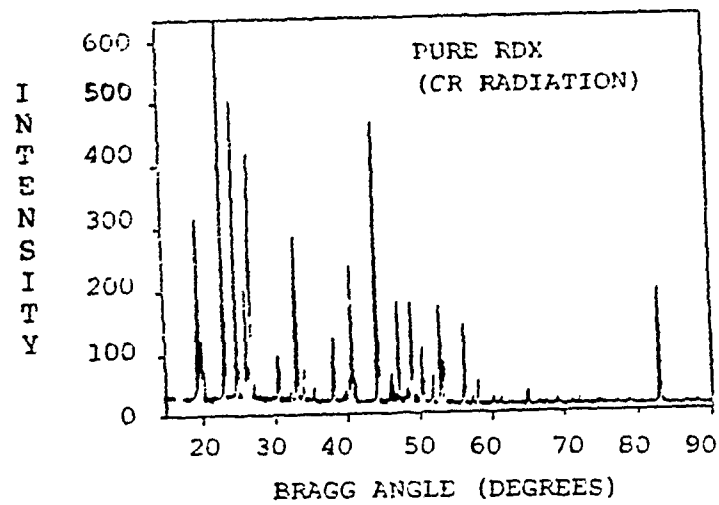
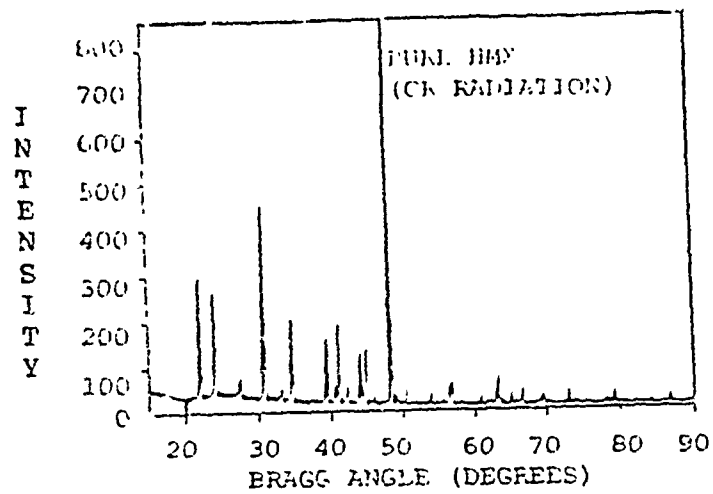


Figure 9 Rapid X-ray Diffraction Pattern of HMX and RDX.

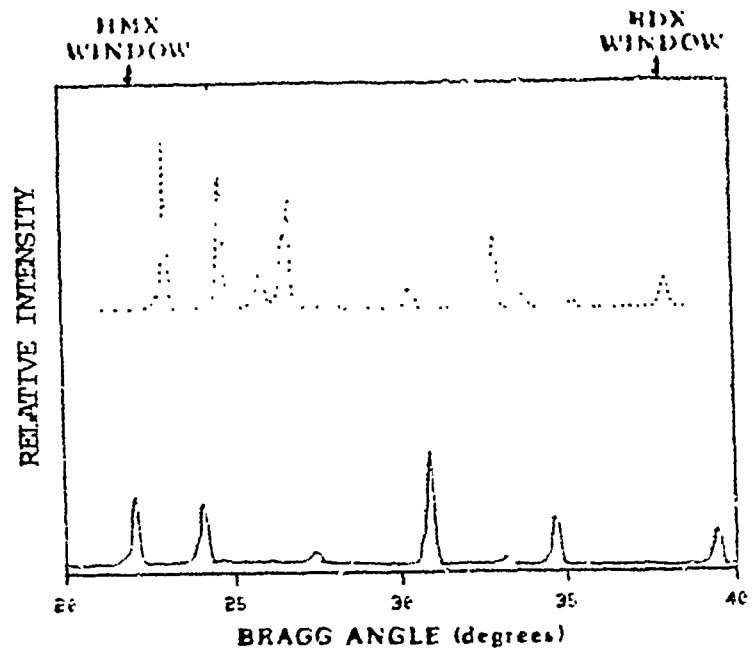


Figure 10 Showing Partial X-ray Diffraction Profiles to RDX & HMX with Appropriate Windows for Constituent Phase Identification and Composition Analysis.

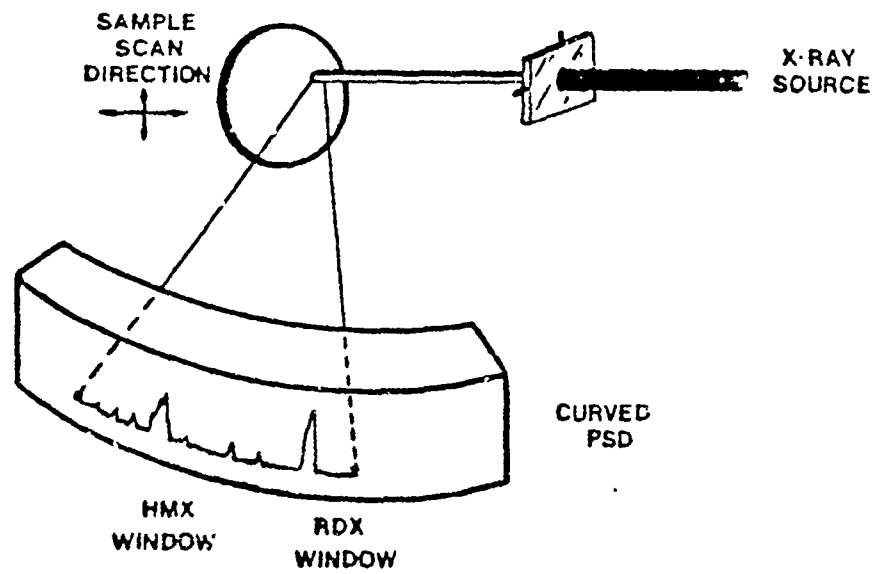
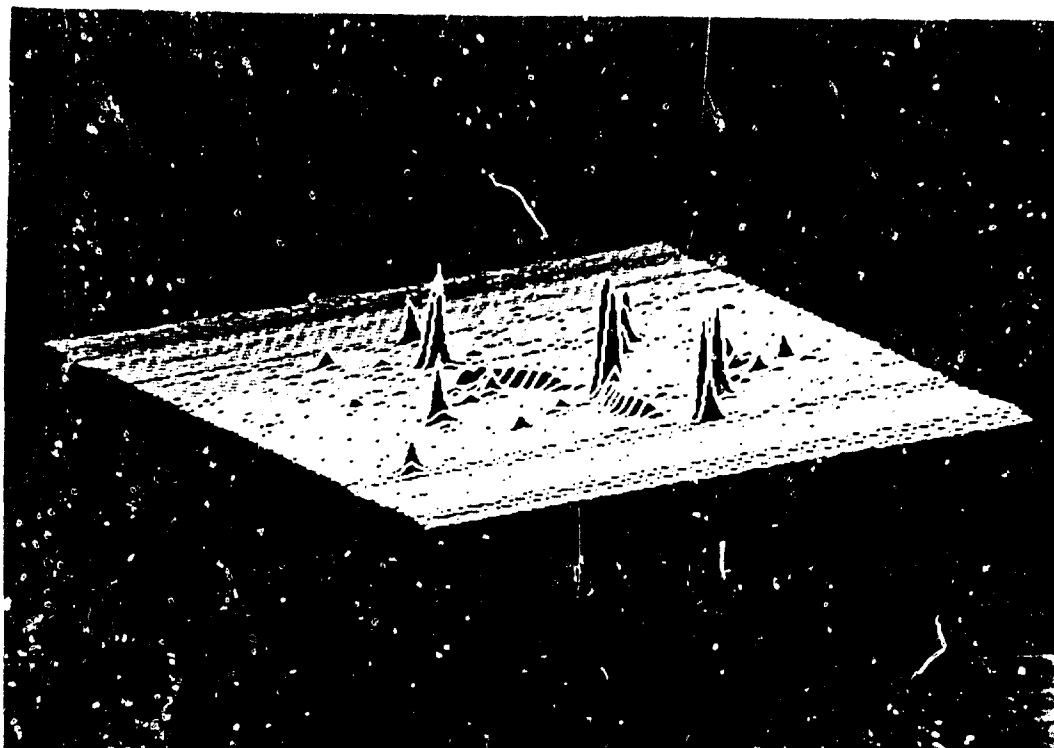
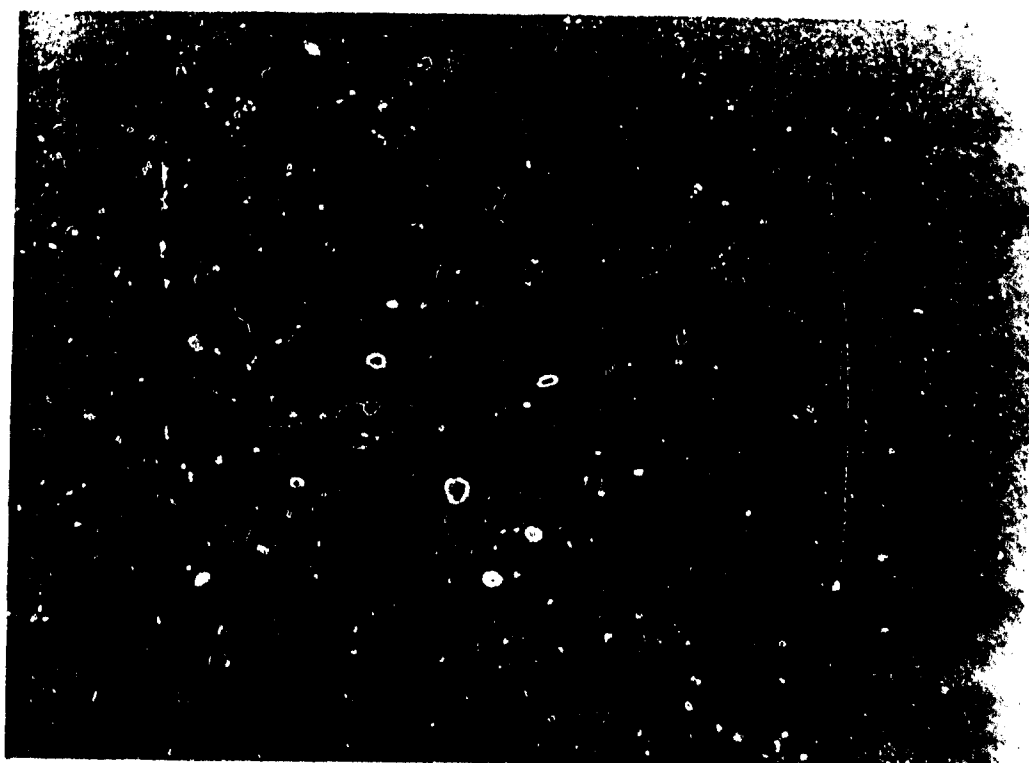


Figure 11 Schematic of Proposed System.

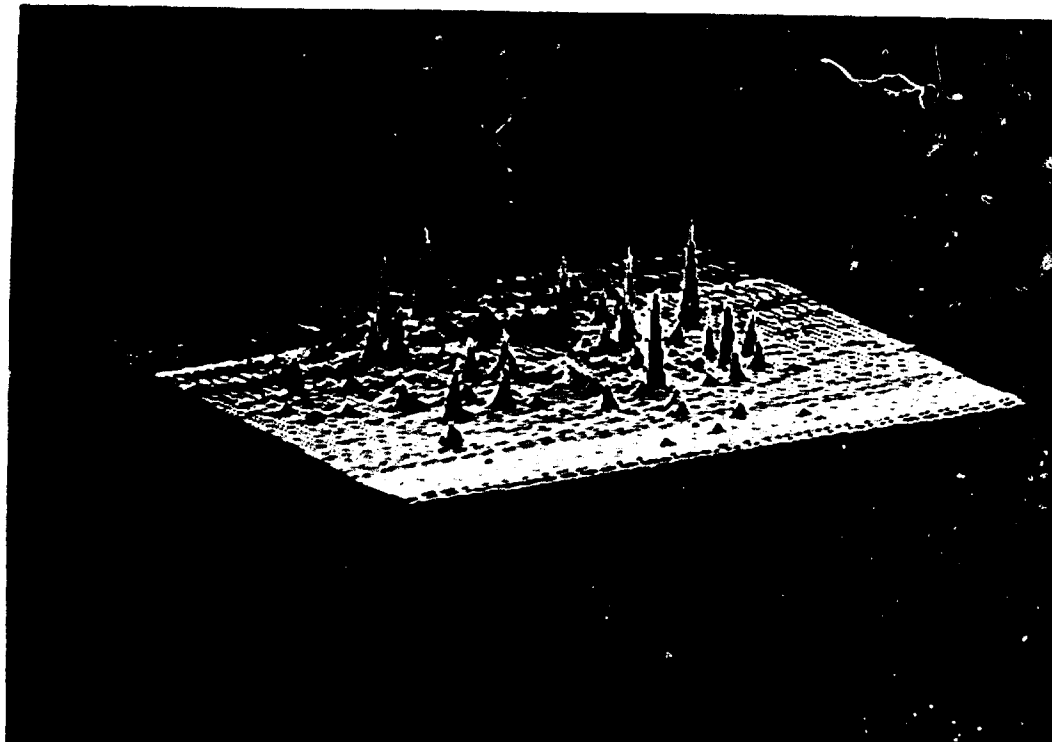


3-D Perspective



Pseudo Color

Figure 12a Real Time Laue Diffraction Pattern from Sugar Particles  
74-149 $\mu$ m.

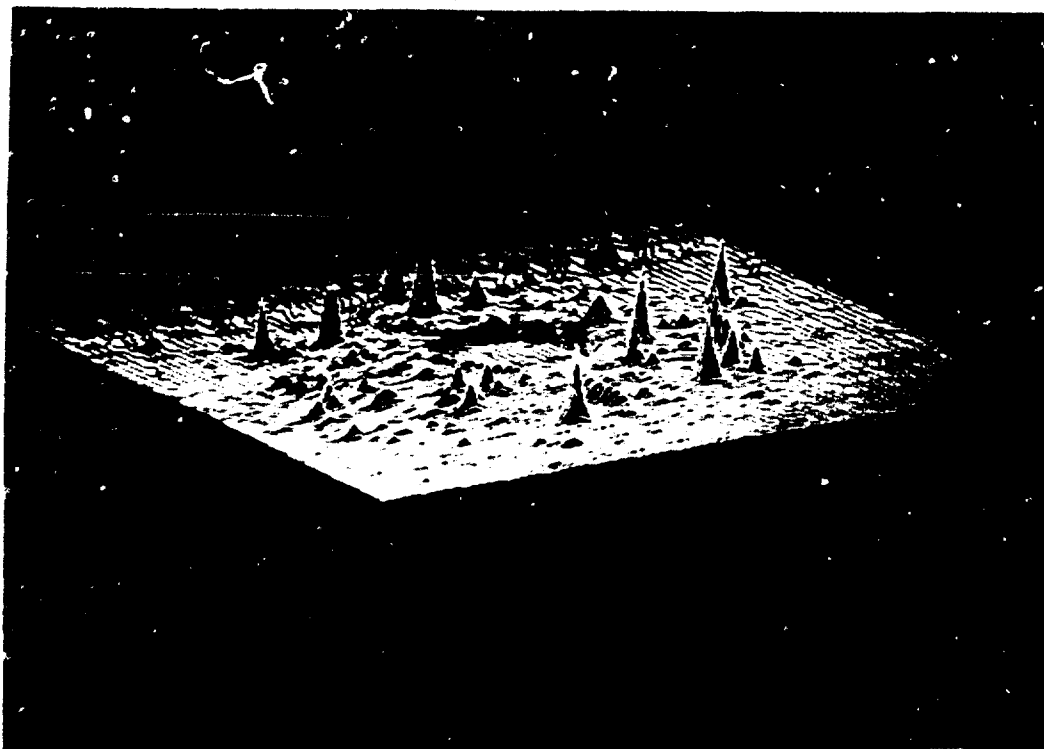


3-D Perspective

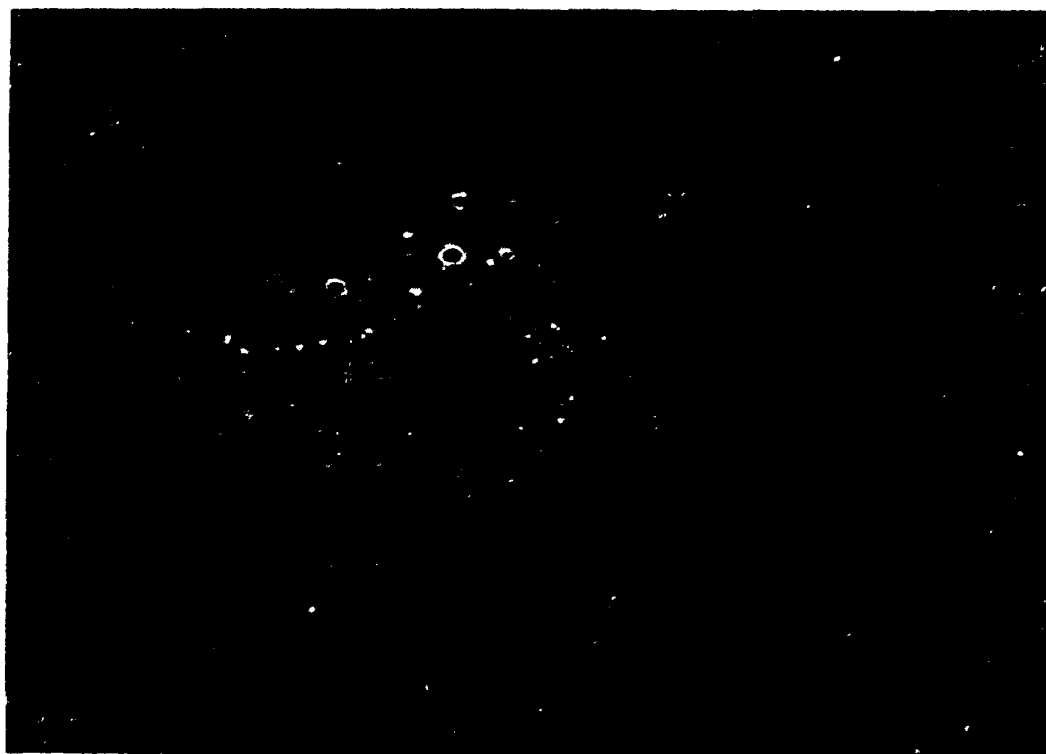


Pseudo Color

Figure 12b Real Time Laue Diffraction Pattern from Sugar Particles  
44-74 $\mu$ m.



3-D Perspective



Pseudo Color

Figure 20 Real Time Laser Diffraction Patterns from Sugar Particles  
0-4  $\mu$ m.

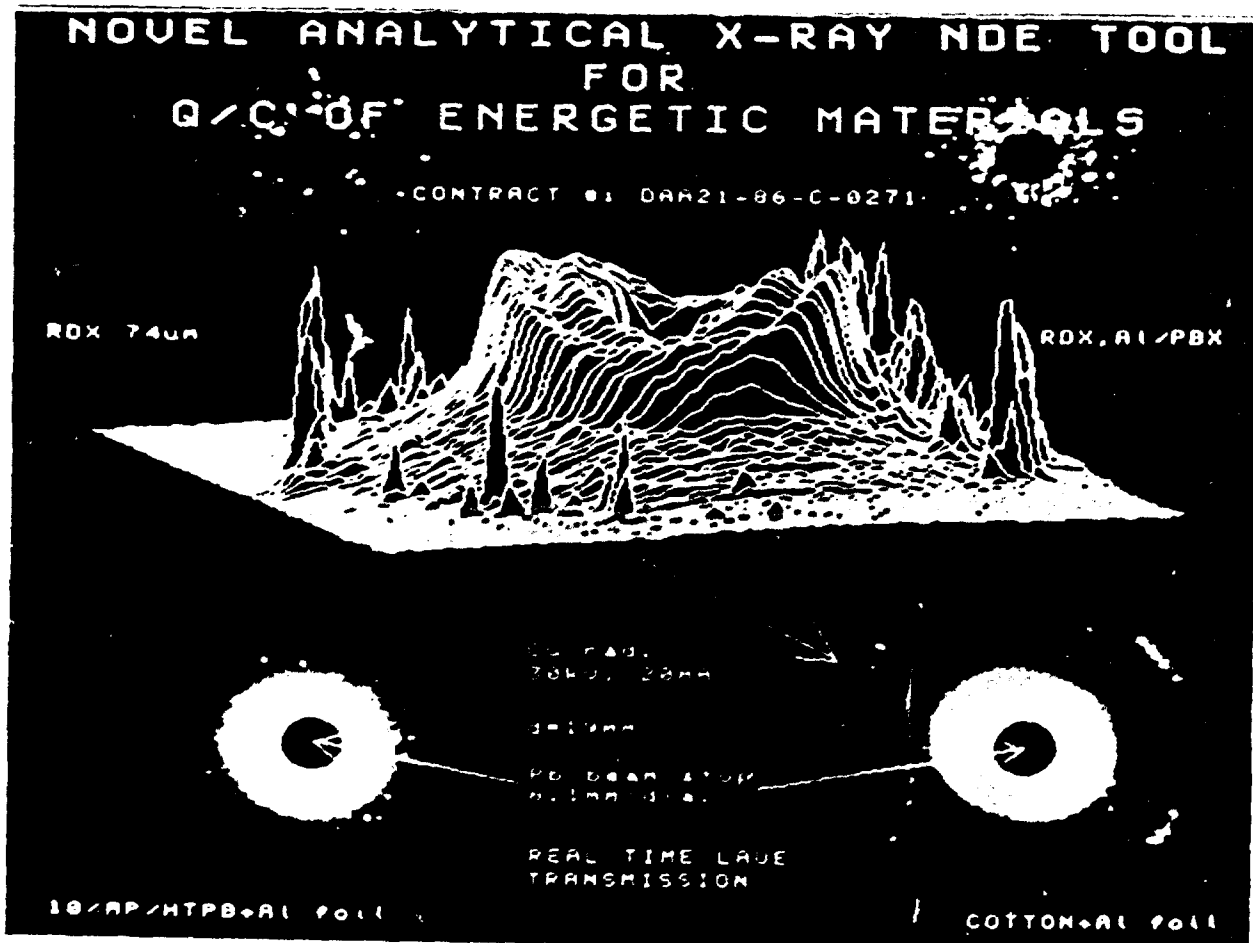


Figure 13a Real Time Transmission Laue of Several Propellant Composites, 74 $\mu$ m ROX, ROX and Al Composites in PBX, 10% Al/HTPB Composite.

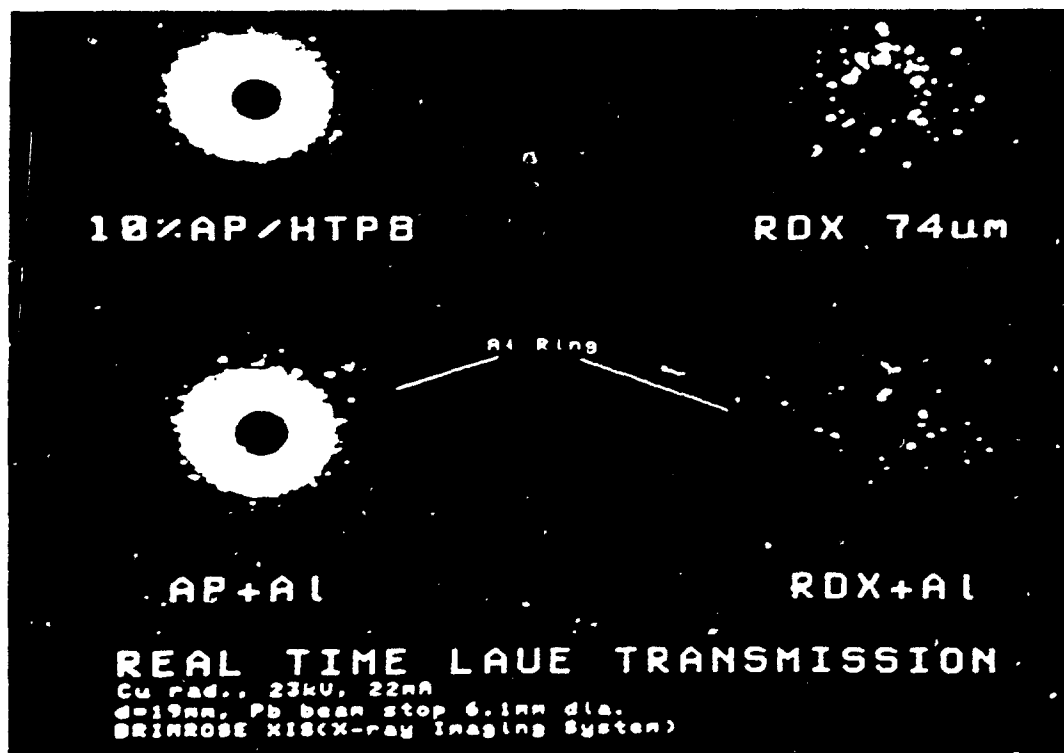
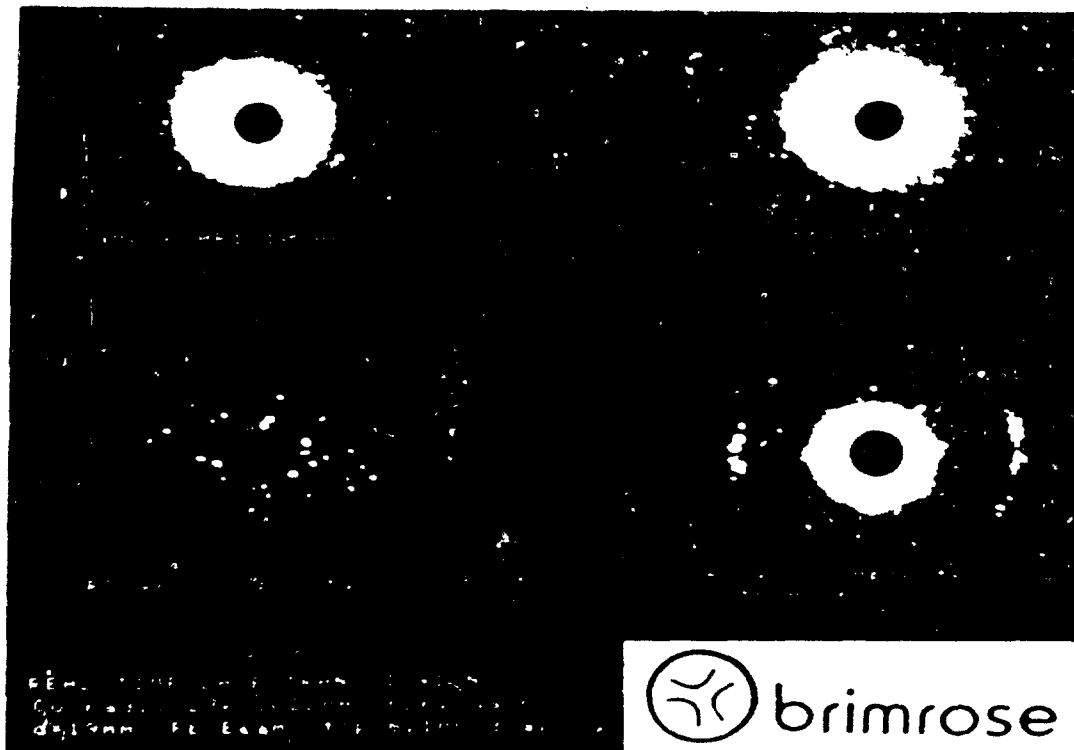


Figure 13b Real Time Transmission Laue of Several Propellant Composites.

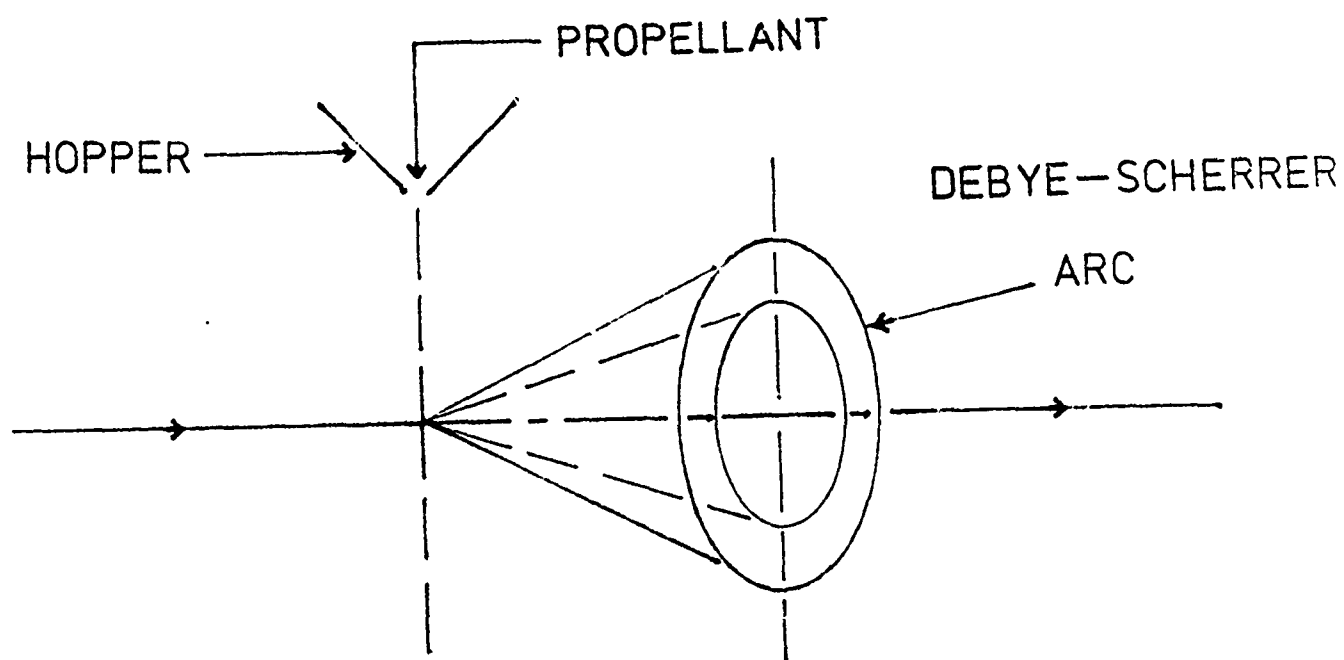


Figure 13c REAL TIME TRANSMISSION LAUE

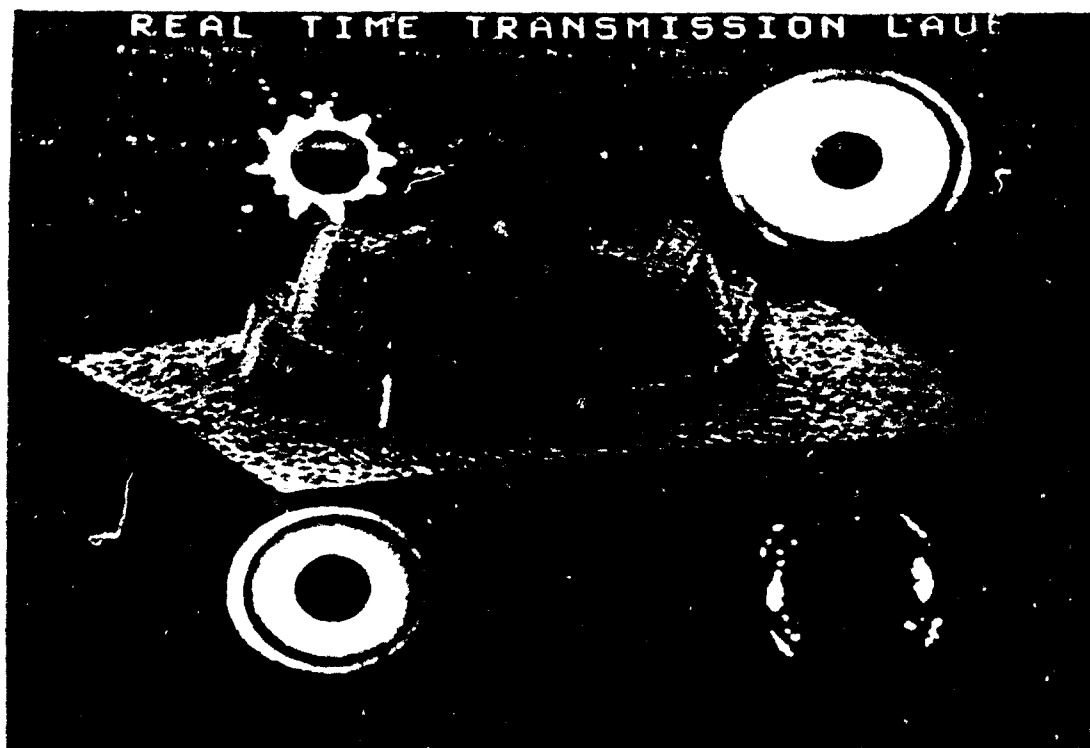


Figure 14 Late Transmission Image from an Al Foil (Reynolds Wrap).

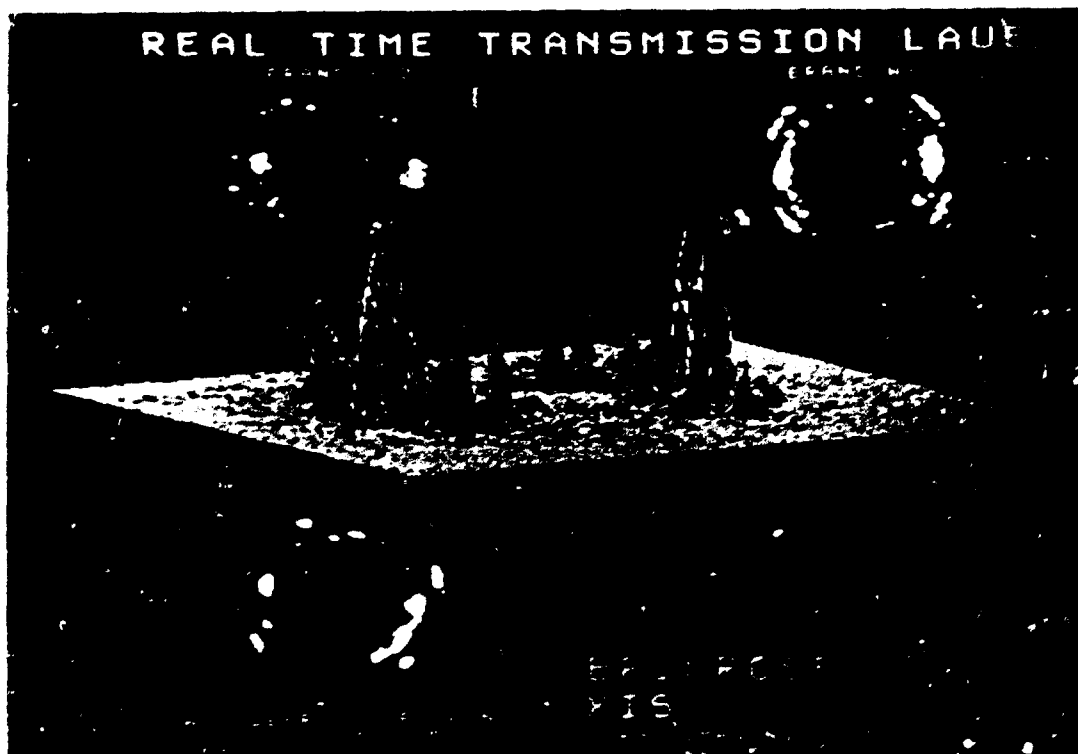


Figure 15 Depiction of the X-ray Pattern from an Al, Cu, Brass & Ni Foils.

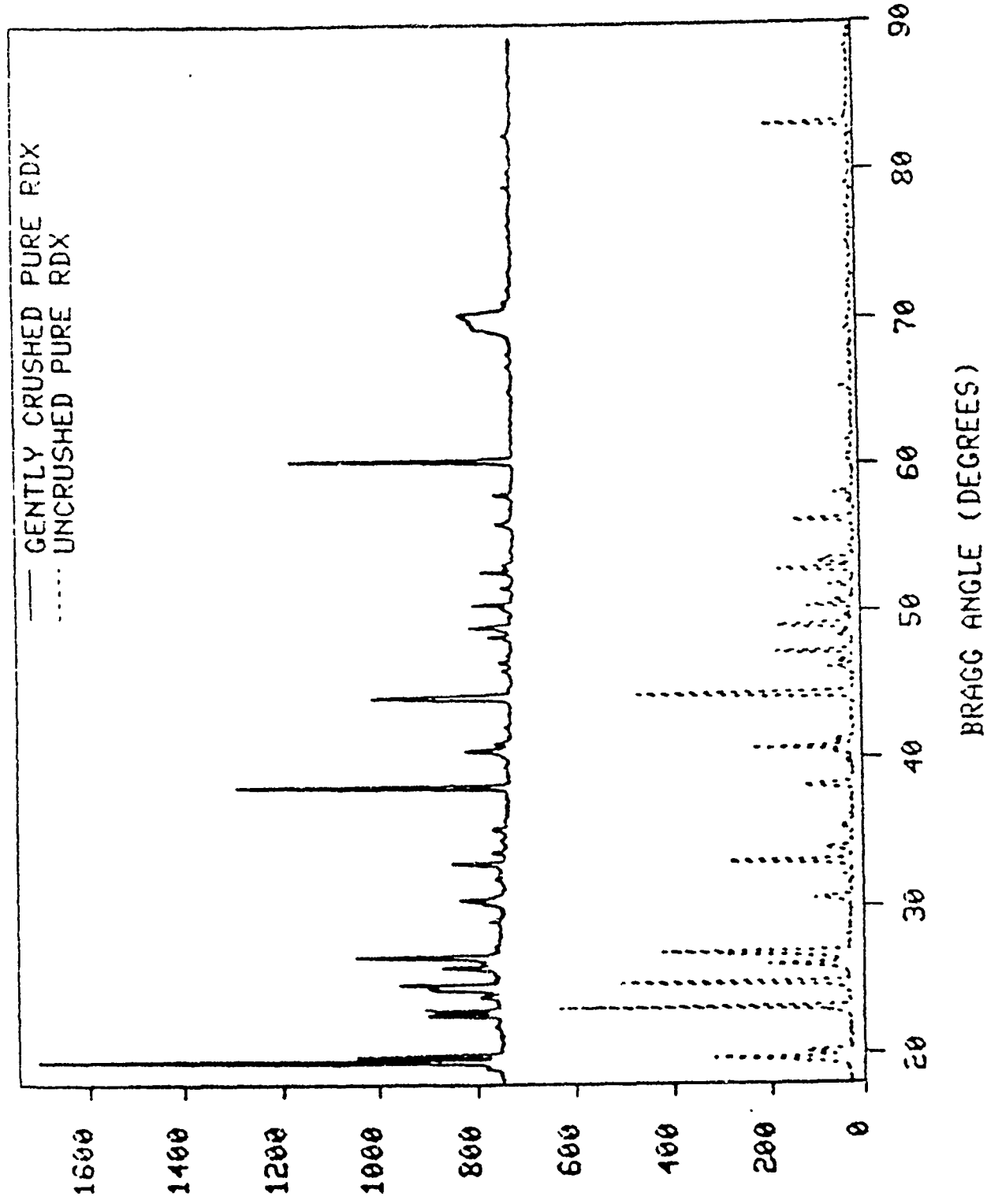


Figure 16a EFFECT OF CRUSHING ON PURE RDX (Cr RADIATION)

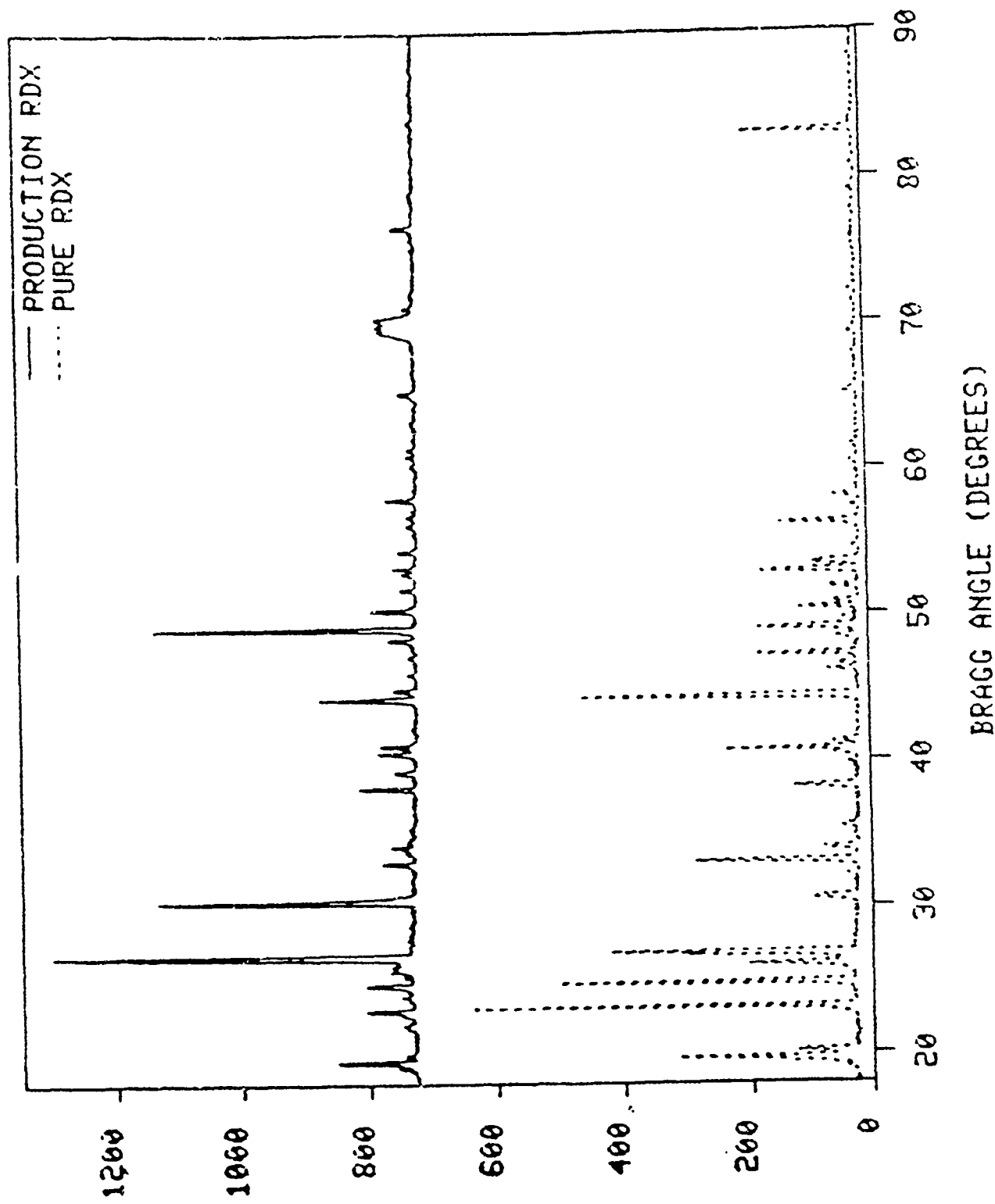


Figure 16b PRODUCTION RDX (LOT X661) VS. PURE RDX

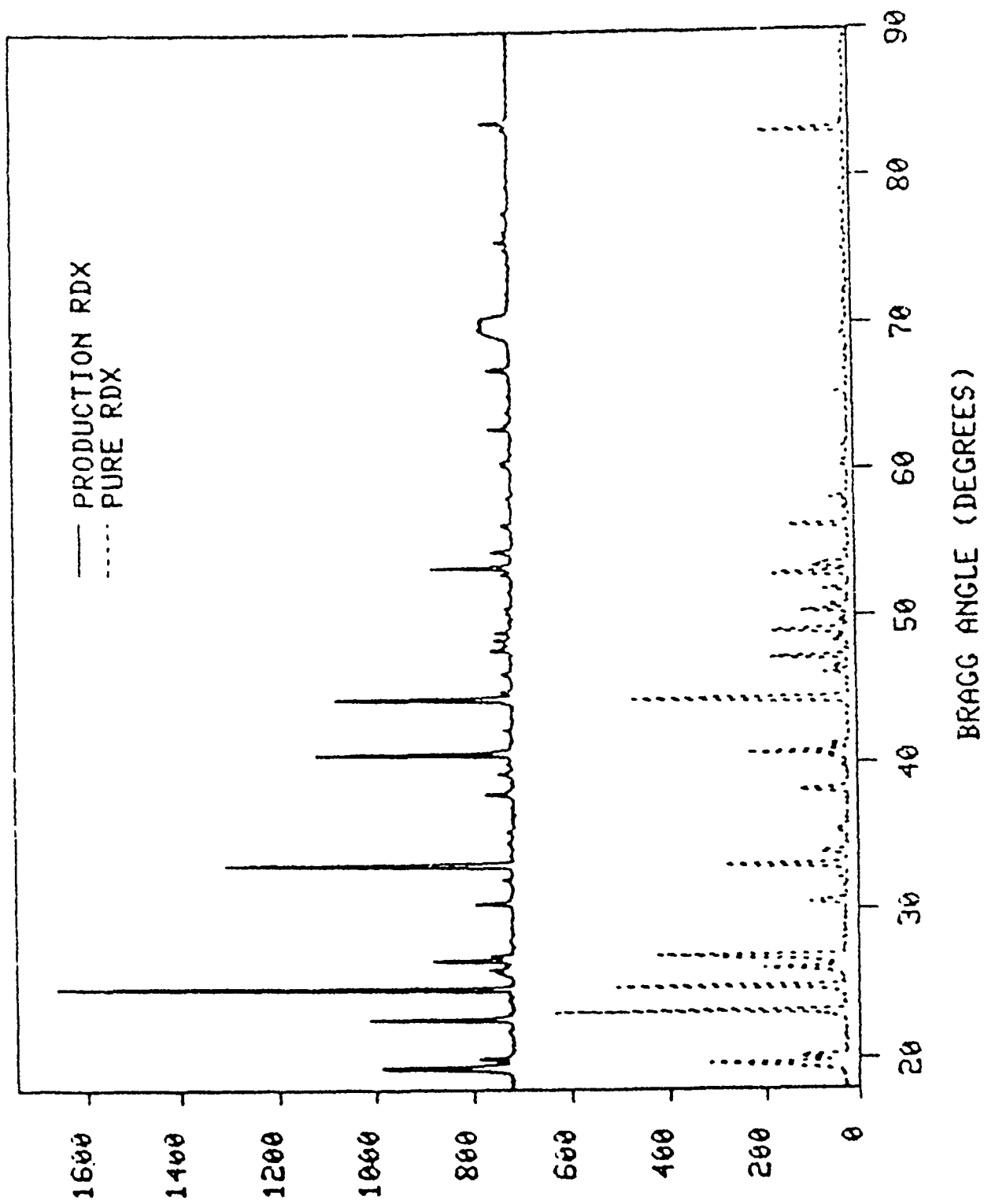


Figure 16c PRODUCTION RDX (LOT A597) VS. PURE RDX

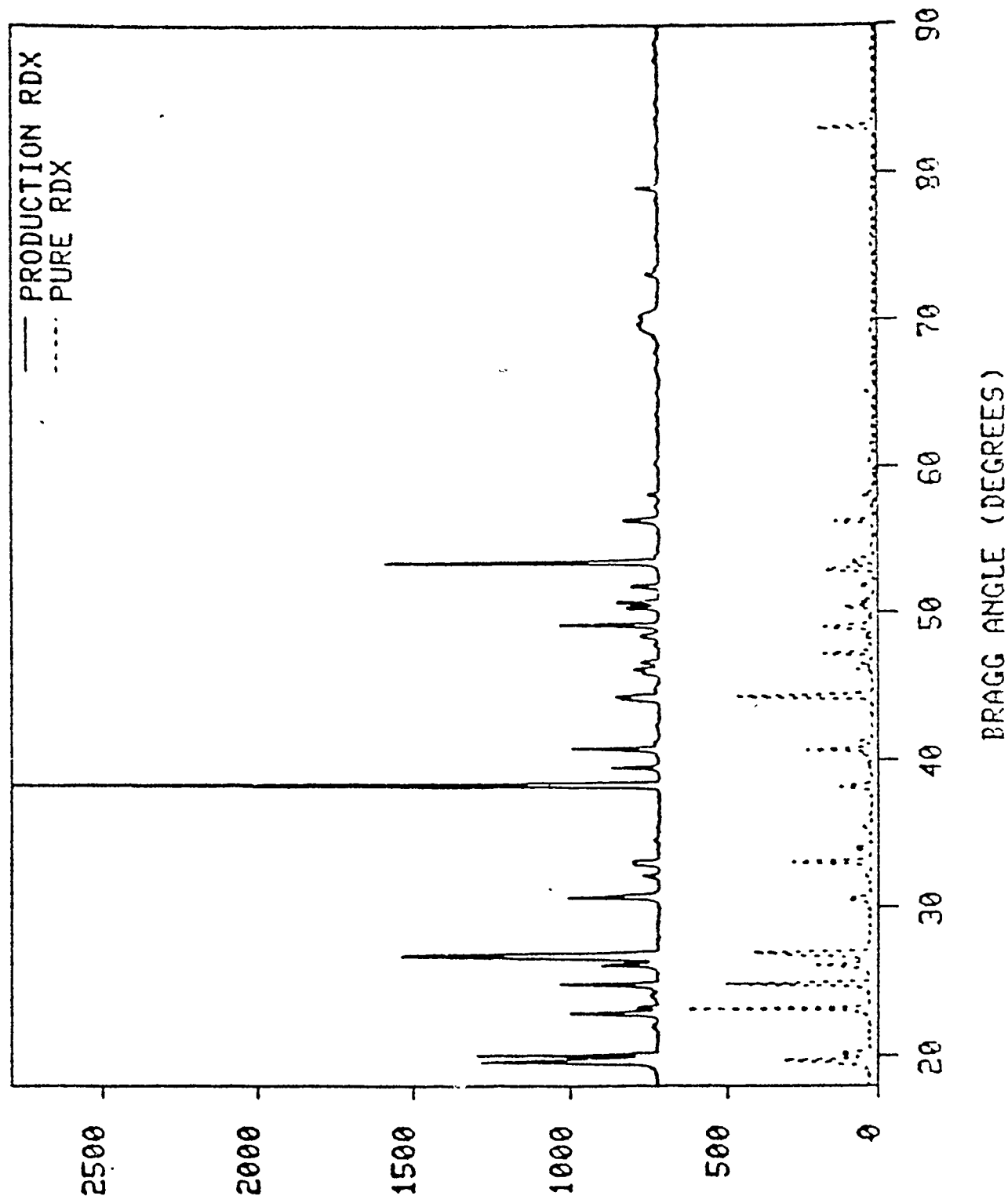
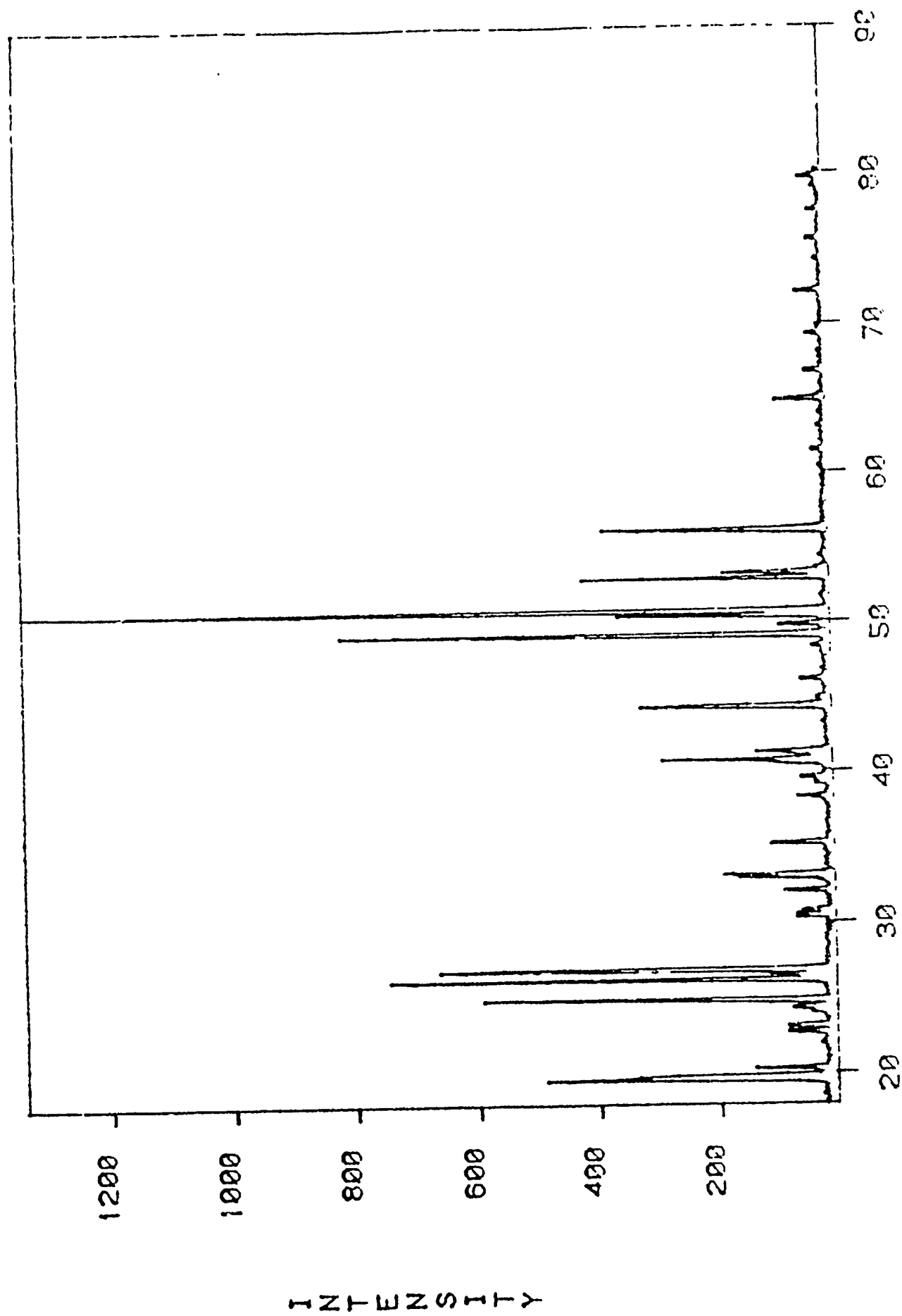


Figure 16d PRODUCTION RDX (LOT A984) VS. PURE RDX



BRAGG ANGLE (DEGREES)

Figure 16e RDX SAMPLE LOT78 (CR RADIATION)



DISTRIBUTION LIST

Commander  
Armament Research, Development  
and Engineering Center  
U.S. Army Armament, Munitions  
and Chemical Command  
ATTN: SMCAP-MSI (5) (Bldg 59)  
SMCAR-AEE-WW (5)  
Picatinny Arsenal, NJ 07806-5000

Commander  
U.S. Army Armament, Munitions  
and Chemical Command  
ATTN: AMSMC-GCL (D)  
Picatinny Arsenal, NJ 07806-5000

Administrator  
Defense Technical Information Center  
ATTN: Accessions Division (12)  
Cameron Station  
Alexandria, VA 22304-6145

Director  
U.S. Army Material Systems  
Analysis Activity  
ATTN: AMXSU-MP  
Aberdeen Proving Ground, MD 21005-5066

Commander  
Chemical Research, Development  
and Engineering Center  
U.S. Army Armament, Munitions  
and Chemical Command  
ATTN: SMCCR-MSI  
Aberdeen Proving Ground, MD 21010-5423

Commander  
Chemical Research, Development  
and Engineering Center  
U.S. Army Armament, Munitions  
and Chemical Command  
ATTN: SMCCR-RSP-A  
Aberdeen Proving Ground, MD 21010-5423

Director  
Ballistic Research Laboratory  
ATTN: AMXBR-OD-ST  
Aberdeen Proving Ground, MD 21005-5066

Chief  
Benet Weapons Laboratory, CCAC  
Armament Research, Development  
and Engineering Center  
U.S. Army Armament, Munitions  
and Chemical Command  
ATTN: SMCAR-OCB-TL  
Watervliet, NY 12189-5000

Commander  
U.S. Army Armament, Munitions  
and Chemical Command  
ATTN: SMCAR-ESP-L  
Rock Island, IL 61299-6000

Director  
U.S. Army TRADOC Systems  
Analysis Activity  
ATTN: ATAA-SL  
White Sands Missile Range, NM 88002